

國立臺灣大學生物資源暨農學院

植物病理與微生物學系

碩士論文

Department of Plant Pathology and Microbiology

College of Bioresources and Agriculture

National Taiwan University

Master Thesis

木材腐朽菌新型基礎過氧化酶基因特性及親緣分析
Demonstrating of novel basal peroxidases (BaPs) in wood
brown and white rot fungi based on gene characterization
and phylogenetic analysis

賴瑞亞

Jui-Ya Lai

指導教授：曾顯雄博士

Advisor: Shean-Shong Tzean, Ph.D.

中華民國 101 年 6 月

June, 2012

Acknowledgment

對於在這襤褸路途上支持我幫助我的人們，謹致上最深的謝意。

我的老闆曾顯雄老師，承蒙多年照顧，遺憾沒有做到最好；夜半三更仍然努力的身影一直是激勵我向前的力量，謝謝老師。感謝劉瑞芬老師、安寶貞老師、袁國芳老師及胡哲明老師對論文的針砭指導。

R323 的伙伴們，能擁有繽紛有趣充滿張力的五年實驗室生活，開心有你們一路相伴，那些開心的憤怒的悲傷的，隨著時間遠颺，留下的都是美好回憶。尤其感謝三年來的好搭檔阿達利以及子禾大師兄。

植微 B94 的損友兼戰友們，青春彷彿揮霍不完，即便大家各分西東，偶然聚首卻還是會因為老掉牙笑點而會心一笑。這三年來若少了互相宣洩咒罵，分享快樂，討論 data，切磋方法；研究路迢迢無以為繼。

植昆女籃的好姊妹，能一起在球場上奔馳追逐勝利，真是人生中最暢快的美好時光；田阿 tra、涵文跟岱樺，七年來承蒙學姊各方面的照顧跟提攜，謝謝你們帶領我認識在球場之外的浩瀚穹蒼。

Dr. Chu, 這段黎明前最黑暗的天堂路，我不是孤獨的。

Ned, thanks for all you did for the thesis.

鍾嘉綾老師，吃東西，很棒吧！

Ino'u aveoveoyu

賴瑞亞

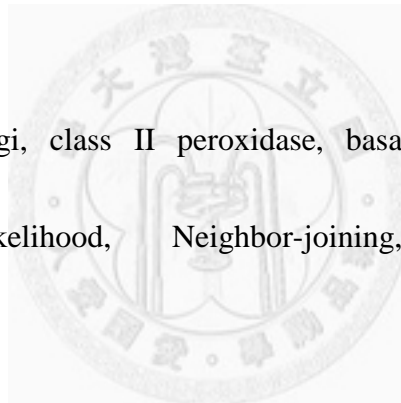
Tanivu Peongsi

Abstract

In light of our previous discovery indicating the existence of a novel lignolytic peroxidase in several wood brown rot fungi (Huang et al. 2009, Huang and Tzean, data unpublished), study on the novel basal peroxidases (BaPs) of additional brown rot and white rot Basidiomycetes was initiated. By degenerate primers, gene encoding the putative novel peroxidase was cloned from *Antrodia salmonea* and *Laetiporus sulphureus*. The coding sequences harbored 1,363 and 1,278-bp in length, respectively, and both were interrupted by 10 introns. Further analysis of the BaP amino acid sequence of *L. sulphureus* showed the high similarity to manganese peroxidase (MnP), and also the presence of unpaired metal regulatory elements (MREs) on the promoter region. The result of quantitative RT-PCR (qRT-PCR) revealed 3.5 times more *BaP* transcripts while augmented with 180 μM Mn^{2+} in the initial 24 hr compared with the control. One copy of *BaP* was shown by Southern blot. Further phylogenetic analysis of the class II fungal peroxidases of 153 taxa represent in Agaricomycetes or Ascomycete by maximum-likelihood (ML), Neighbor-joining (NJ) and Bayesian inference (BI), indicated that BaP, which clearly separated from MnP, lignin peroxidase (LiP) and versatile peroxidase (VP) clades, not only present in the tested brown rot- (A.

cinnamomea, *A. salmonea*, *L. sulphureus*, *Gloeophyllum trabeum* and *Fomitopsis pinicola*), but in a small group of white rot (*Ganoderma lucidum*, *G. australe*, *Phellinus noxius*, *Trametes versicolor*, *Agaricus bisporus* and *Pycnoporus sanguineus*) Agaricomycetes and even Ascomycete (*Ophiostoma quercus*). The phylogenetic tree topology implicated the possible evolutionary route of BaP diverged toward MnP, LiP and VP.

Keywords: wood rot fungi, class II peroxidase, basal peroxidase, homologous modeling, Maximum-likelihood, Neighbor-joining, Bayesian inference



摘要

木材腐朽菌依其具有降解木質素之能力與否可分為白腐菌與褐腐菌。前人研究指出在白腐菌之外，屬於褐腐菌之牛樟芝 (*Antrodia cinnamomea*) 亦具有木質過氧化酶之部份活性。而木質過氧化酶之有無為白腐菌及褐腐菌分類依據之一，牛樟芝具有木質過氧化酶此一事實強烈挑戰此論點。本研究以此為出發點，嘗試選殖出它種褐腐菌之木質素過氧化酶。藉由簡併式引子對自數種木材腐朽菌中增幅出具相當保守性之木質素過氧化酶基因片段。此外以末端選殖技術 (Rapid amplification of cDNA Ends, RACE) 選殖出 *Laetiporus sulphureus* 及香衫芝 *Antrodia salmonea* 之 cDNA 全長，分別為 1,278 及 1,378 個鹼基對。選定 *L. sulphureus* 做進一步之分析發現，其基因長度為 1,920 個鹼基對並帶有十個內插子 (intron)，拷貝數 (copy number) 為一。並以熱不對稱交錯 PCR (tail-PCR) 獲取其啟動子 (promoter) 區域並進行分析，發現有兩個非成對之金屬調節元件 (metal regulatory elements, MREs) 之轉錄因子結合位點於此木質素過氧化酶基因上游，此為錳依賴型過氧化酶 (Mn-dependent peroxidase, MnP) 之特徵，此外也其具有與 MnP 較高之序列相似性。為探討其與基因表現之關聯，進行即時定量 PCR (quantitative real-time PCR) 發現於高濃度錳離子 (180 μ M) 處理下基因之表現量較控制組高 3.5 倍，但此結果與 MnP 基因受錳離子催化結果相較較不明顯。為進一步探討此基因之屬性，從譜系分析上切入，將自褐腐菌與白腐菌以及子囊菌上選殖之過氧化酶基因進行分析，採用最大似然法 (Maximum likelihood)，鄰近相接法 (neighbor-joining) 及貝葉氏導出式分析 (Bayesian inference) 建構第二類過氧化酶 (class II peroxidase) 之親緣樹。結果指出基礎過氧化酶 (basal peroxidase, BaP) 成在第二類過氧化酶中成一單系群 (monophyletic group)，此類過氧化酶是否參與木質素降解功能尚未知。三種方法建構之演化樹樹型並不完全相同但分群近似，皆支持 BaP 相較於其餘類型之第二類過氧化酶較為原始，可能為現有木質分解過氧化酶之起緣酶。由於 BaP 不僅存在於擔子菌 (Basidiomycetes)，也在

子囊菌 (Ascomycetes) 中被發現，說明木質素過氧化酶之特化應在擔子菌自子囊菌中演化之後發生。

關鍵字：木材腐朽菌，第二類過氧化酶，基礎過氧化酶，同源模擬，最大似然法，鄰近相接法，貝葉氏導出法



Content

Acknowledgment.....	壹
Abstract.....	I
摘要	III
Introduction	1
Structure of wood	1
Wood rot fungi.....	2
Brown rot fungi	3
Lignin and lignin degrading oxidative enzymes.....	5
Class II peroxidase, ligninase, PODs	7
Phylogenetic studies of class II peroxidase, PODs	11
Materials and Methods	14
Fungal isolates, culture conditions and cultures preservation.....	14
Cloning of wood decay fungi partial putative <i>BaP</i> gene.....	14
Genomic DNA extractions	15
<i>L. sulphureus</i> <i>BaP</i> cDNA: full-length cloning and analysis.....	16
RNA extraction and rapid amplification of cDNA ends.....	16
Primer design.....	17

Rapid amplification of cDNA ends (RACE)	18
Promoter region of <i>MnP</i> gene cloning and analysis.....	18
Gene copy number determination: Southern blot analysis	19
Induction for <i>MnP</i> gene expression and analysis	21
Culture conditions of <i>L. sulphureus</i>	21
Extraction of RNA under different incubation conditions and time course	22
Reverse transcriptase-polymerase chain reaction (RT-PCR)	23
Real-time quantitative PCR (qPCR) analysis.....	23
Modeling the 3-D molecular structure of basal peroxidase.....	24
BaP sequences alignment and phylogenetic tree construction	25
Sequences collection and alignment.....	25
Phylogenetic tree construction by Maximum likelihood (ML) method	26
Phylogenetic tree construction by Neighbor-joining (NJ) method.....	26
Phylogenetic tree construction by Bayesian inference method.....	26
Results	29
Discussion.....	36
Reference	46
Appendix	84

List of Tables and Figures

Table 1. Fungal species used in basal peroxidase gene cloning and characterization....	61
Table 2. Primers used in this study	62
Table 3. Reaction parameters for the tail-PCR	63
Fig. 1. Putative basal peroxidase gene cloned from brown rot and white rot fungi by degenerate primers.....	64
Fig. 2. Putative basal peroxidase gene cloning from <i>Ophiostoma quercus</i> by degenerate primers.....	65
Figure 3. Traits of cloned basal peroxidase gene in target fungal species.....	66
Fig. 4. The gene structure of <i>Laetiporus sulphureus</i> (Ls) <i>LsBaP</i>	67
Fig. 5. Nucleotide and translated amino acid sequences of basal peroxidase gene of <i>L.</i> <i>sulphureus</i> (<i>LsBaP</i>).	70
Fig. 6. The exon / introns distribution of basal peroxidase, lignin peroxidase, manganese peroxidase, CiP and ARP in nine white and brown rot Basidiomycetes:	71
Fig. 7. The analysis of <i>LsBaP</i> promoter.	72
Fig. 8. The quantitative RT-PCR analysis of <i>LsBaP</i>	73

Fig. 9. The comparison of backbone structure between putative of LsBaP (up) and versatile peroxidase of *P. eryngii* (down) 75

Fig. 10. The comparison of ligand binding site between *P. eryngii* versatile peroxidase and the *L. sulphureus* novel peroxidase..... 77

Fig. 11. Phylogenetic tree revealed by Maximum likelihood (ML) method. 79

Figure 12. The Phylogenetic tree disclosed by Neighbor-joining (NJ) method..... 81

Figure 13. The phylogenetic tree showed by Bayesian inference (BI) method. 83



Introduction

Structure of wood

Wood, a basic structural component of forest ecosystems that supports diverse organisms, also contributes important ecological and sociological benefits, such as building material, fuel, soil composition, wildlife habitat, etc. Furthermore, forest-derived wood provides an essential renewable natural resource for human use. Lignocellulose, which constitutes wood biomass, contributes most renewable organic resource found on earth (Abbasi et al. 2010). Because of fossil fuel depletion and concerns about global climate change, scientists continue to seek alternative energy sources. Plants use solar energy to fix carbon to synthesize carbohydrates through photosynthesis. The polymerized complex carbohydrates are further modified and formed the lignocellulosic compounds (cellulose, hemicellulose, and lignin), that form a thick wall layer around the plant cell (Rubin 2008).

The rigid structure of woody plants is mainly formed via the vascular cambium, located between the phloem and xylem. The vascular bundles consist of inner xylem, outer phloem, and cambium, which are arranged in cylindrical fashion around the stem. Each woody plant cell is separated by the middle lamella, which is pectin, i.e. lignin-rich structure. A thick primary cell wall and secondary cell wall are formed

outside the plasma membrane that surrounds the cytoplasm. Most woody plants generally contain a two-layer, cell-wall structure, with the exception of some conifers that contain only a primary cell wall. Compared with the relatively simple primary cell wall, the secondary cell wall is composed of three layers: S1, S2 and S3. These layers possess different characteristics in chemical structure. The major components of cell wall are cellulose, hemicellulose, and lignin. Cellulose constitutes approximately 40-55% followed by approximately 25-40% hemicellulose and 18- 33% lignin of the mass within plant cell walls (Eaton et al. 1993). Wood is typically classified as hardwood or softwood, depending on the compositions of the cell wall as well as vascular structure. Compared to softwoods, hardwoods have a more complex anatomical composition that contains several cell types, such as vessels, parenchyma, and fibers. In contrast, softwoods are predominately comprised of tracheids and transverse ray cells (Eaton et al. 1993).

Wood rot fungi

In fungi particularly in Basidiomycota, in addition to a few bacteria, are the dominant organisms able to degrade woods by chemical and physical mechanisms. The cell wall, which surrounds the wood cell, constitutes a major barrier to wood biodegradation. Especially of lignification for woody plants, providing a solid physical

obstacle and a waterproof layer impede biotic and abiotic degradation (Hon et al. 2001). Microbes must penetrate the durable lignin matrix of the cell wall before cellulose or hemicellulose can be efficiently hydrolyzed and accessed as a carbon source. Wood-degradating fungi are generally classified as white-rot fungi or brown rot fungi, depending on their capability to degrade lignin. White rot fungi, which have the capacity to depolymerize and mineralize lignin, have a long history of exploration (Goodell et al. 2003). It has been generally recognized that white rot fungi are capable of depolymerizing lignin and gaining physical access to the cellulose. Although brown rot fungi are evolutionarily related to white rot fungi, they lack the capacity to mineralize lignin. To better understand the genes and enzymes involved in lignin-degrading, whole genome sequencing of a model white rot fungus, *Phanerochaete chrysosporium* was completed in 2004 for, using a shotgun strategy (Martinez et al. 2004).

Brown rot fungi

Brown rot fungi have been generally regarded as unable to degrade lignin, although they maybe able to modify it slightly. These fungi possess of this compacity belong to the phylum Basidiomycota, and are well-represented in the family Polyporaceae (Schwarze et al. 2000). Compared with white rot fungi, wood degrading

mechanisms of brown rot fungi remain relatively ill-defined. According to previous studies shown that, brown rot fungi are active in wood decay of conifers, exclusively (Gilbertson 1980, Hibbett et al. 2001). This phenomenon is especially interesting, given that brown rot fungi are considered to have evolved repeatedly from white rot fungi, which able to sustain on conifers and hardwoods as well (Hibbett et al. 2001). Wood degrading mechanisms of brown rot fungi seem relatively simplified, in contrast to white rot fungi innates diverse mechanisms to degrade wood. In order to breakdown cellulose and hemicelluloses, growing hyphae must penetrate through the secondary cell wall to gain access to the cellulose-rich S₂ layer inside. Preferential degradation occurs to the S₂ layer because the lignin content of the S₂ layer is lower than that of S₁, S₃, and lignin-dense middle lamella (Sachs et al. 1963). Hemicelluloses surrounding the cellulose are usually decomposed first, accompanied by partial lignin modification. Subsequently, cleavage of cellulose takes place rapidly. Cellulose degradation by brown rot fungi occur provided that other wood components i.e. hemicelluloses, lignin, or even pectin are present in the vicinity (Enoki et al. 1988, Goodell 2003). After the lignin-modificated, some phenolic derivatives are generated, that can play a key role in Fenton-based reactions (Goodell et al. 1997). Because white rot fungi possess intrinsic wood degrading enzymes that exceed the size of pores in the cell wall, wood degradation can only occur from the outside. In contrast, brown rot fungi accomplish

delignification through a low molecular weight decay system. Therefore, brown rot fungi can cause rapid wood-strength loss, while white rot fungi cause a more gradual loss of wood strength (Goodell 2003). Brown rot fungi produce little or no lignin-degrading enzymes, so the remaining rotten wood is reddish-brown in color. Strong evidence do support the existence of ligninase in brown rot fungi is generally lacking: however, more recent study showed that the potential lignin peroxidase (LiP) activity assay for *Polyporus ostreiformis* (Dey et al. 1994) and ligninolytic peroxidase activity in *Antrodia cinnamomea* (Huang et al. 2009) accessed.

Lignin and lignin degrading oxidative enzymes

Lignin, which comprises complex amorphous phenolic biopolymers, is composed of phenylpropane monomers. Of these phenylpropane monomers, coniferyl alcohol is a primary lignin precursor in gymnosperms (softwoods), whereas, p-coumaryl alcohol and sinapyl alcohol are primary lignin precursors in angiosperms (hardwoods) and the Gramineae (Eriksson et al. 1990, Paterson et al. 1984, Sakakibara 1980). The complex structure of lignin is attributed to various linkages derived from diverse reactions. More than two thirds of the phenylpropane monomers are linked by ether bonds or ester bonds (C-O-C), and the remaining monomers are linked by C-C bonds in random fashion. The major linkage type among lignin polymers is β -O-4

ether bonds (Goodell et al. 2003, Terashima et al. 1997).

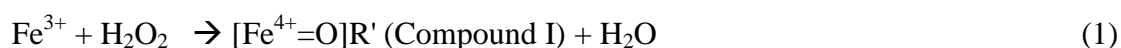
In addition to the linkages among the phenylpropane monomers themselves, the polymerization of lignin also requires other functional groups, such as methoxyl, phenolic hydroxyl, benzyl alcohol, carbonyl, etc. So far, the methoxyl group is the dominant functional group in lignin of both softwood and hardwood (Sjöström 1993).

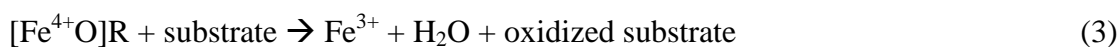
As mentioned previously, white rot fungi have unique lignin-degrading, enzyme systems to catalyze lignin biodegradation. In 2008, Levasseur classified the lignin oxidative enzymes into two sub-families: lignin oxidase (LOs) and auxiliary enzymes (LDAs), depending on whether the enzymatic role in lignin degradation is direct or indirect. Relative to lignin oxidase, auxiliary enzymes, such as aryl-alcohol oxidase, vanillyl-alcohol oxidase, glyoxal oxidase, etc., have low potential oxidative activity. However, lignin oxidase is the primary focus of investigation in this study. Lignin oxidase comprises three sub-families: LO1, LO2 and LO3 (Levasseur et al. 2008). Among these enzyme sub-families, LO2, which contains lignin peroxidase (LiP), manganese peroxidase (MnP), and more recently characterized versatile peroxidase (VP), with being regarded as one the most important lignin-degrading enzymes due to their high redox potential (Levasseur et al. 2008). Although white rot or brown rot fungi can degrade or modify lignin with various mechanisms (LO1, LO2 or LO3), only of the fungi that produce LO2 (true ligninase, fungal class II peroxidase, PODs) are

considered as white rot fungi.

Class II peroxidase, ligninase, PODs

Ligninase of *P. chrysosporium* have been shown to share similar characteristics with general peroxidase, in terms of enzyme kinetics and structure aspects (Kuila et al. 1985, Tien et al. 1986, Tien et al. 1987). As a member of the plant peroxidase superfamily, LiP is a heme protein with single high-spin iron protoporphyrin IX active site (Kuila et al. 1985) that is connected with two histidine units as proximal and distal ligand residues involved in electron transfer (Dunford et al. 1976). The above structure is conserved across most peroxidases classified (Conesa et al. 2002, Poulos et al. 1980, Welinder 1992). For LiP of *P. chrysosporium*, distal His47/Arg43 and proximal His176 participate as axial ligands of the heme, and play critical roles in the oxidation of H₂O₂, respectively (Poulos et al. 1980). Lignin degradation catalyzed by LiP is a H₂O₂-dependent oxidation, and veratryl alcohol (3,4-dimethoxybenzyl alcohol, VA), produced by *P. chrysosporium*, is another key substrate involved in the reaction. In the LiP catalytic cycle, various non-phenolic compounds can also serve as the substrates. The generalized LiP enzymatic reaction can be represented as follows:





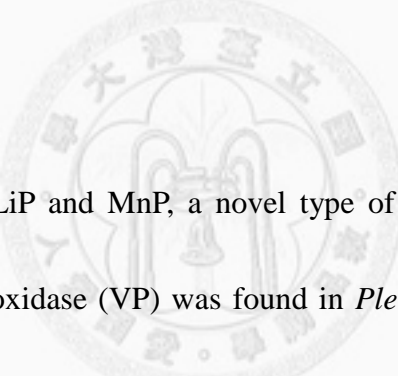
Previous studies have shown that some phenolic compounds, which can inhibit LiP activity, and VA produced by *P. chrysosporium* can act not only as mediators but also as electron donors to reduce compound II to compound III by reduction of H_2O_2 , and after return LiP to its ground state. Moreover, the ability of LiP to oxidize phenolic compounds relies indirectly on the presence of VA (Chung et al. 1995, Harvey et al. 1989, Koduri et al. 1994). In an early study of the VA-binding site, Trp171, C β -hydroxylated tryptophan (Trp171) could serve as “second substrate-binding site,” which is different from other peroxidases (Choinowski et al. 1999). Spin-trapping as well as peptide mapping provided more evidence for critical role of Trp171 in redox catalysis (Blodig et al. 1999).

In addition to LiP, H_2O_2 -dependent oxidase has been found in *P. chrysosporium* by chromatography on blue agarose in 1984 (Kuwahara et al. 1984). This oxidase has almost the same reaction mechanism as LiP, but in this instance, Mn^{2+} acts as the reductant rather than VA, as shown in the following catalytic cycle: native MnP \rightarrow compound I \rightarrow compound II \rightarrow native MnP. The H_2O_2 -dependent oxidase is capable

of oxidizing various substrates including both non-phenolic and phenolic or non-phenolic compounds. Similar to the role played by VA in the LiP-catalyzed reaction, Mn^{2+} can foster the reduction of compound I to compound II, coupling by oxidation of a phenolic compound. Subsequently, Mn (II) in its activated oxidized state could further trigger oxidation of lignin-related compounds, such as guaiacyl and syringyl (Hammel et al. 1989, Wariishi et al. 1988).

Based on crystallographic structure, the MnP has a 43% amino acid sequence identity with LiP isozyme 2 (LiP2). For forming the heme activation site, MnP also has distal His46/Arg42 and proximal His173 similar to other plant and fungal peroxidases. Besides these conserved features, the unique manganese-binding site is formed by three residues: Glu35, Glu39 and Asp179. Based on crystallographic methods (Sundaramoorthy et al. 1994) and site-directed mutagenesis (Kishi, Kusters-van Someren et al. 1996), Mn^{2+} is linked to the pocket through the carboxylate oxygen of these residues, heme propionate oxygen, and two oxygens of water. As shown from E35Q, E39Q and E35Q-D179N mutants, the first-order rate constants were reduced dramatically relative to the wild type (Kishi et al. 1996). Furthermore, a similar study performed in the *Escherichia coli* heterologous expression system also supported the same conclusion (Whitwam et al. 1997).

Previous studies have also focused on how *P. chrysosporium* regulates LiP and MnP activity. The presence of Mn was shown to influence the quantity of VA in *P. chrysosporium*. Mn indirectly regulates LiP activities by influencing endogenous VA production (Mester et al. 1995). Furthermore, it was reported that VA prevents the inactivation of LiP by H₂O₂ (Tonon et al. 1988, Valli et al. 1990). It was suggested that Mn may play a role in stabilization of LiP instead of acting as an inducer (Cancel et al. 1993).



In contrast to typical LiP and MnP, a novel type of fungal class II peroxidase (PODs) called versatile peroxidase (VP) was found in *Pleurotus eryngii* (Martinez et al. 1996, Ruiz-Duenas et al. 2001, Ruiz-Dueñas et al. 1999) and *Bjerkandera* spp. (Mester et al. 1998). Because its Mn-binding site comprises Asp175, Glu40 and Glu36, it has the capacity to oxidize Mn(II) to Mn(III). And VP also with Trp164 (in the same position as Trp171 in *P. chrysosporium*) is able to use VA as substrate through the electron-transfer pathway as well. However, relative to MnP, VP oxidizes Mn(II) with a lower K_m value, which indicates that VP has higher substrate affinity than typical MnP (Heinfling et al. 1998). Above all, VA has two substrate binding site innated by LiP and MnP respectively.

With respect to influences of the nutritional aspects of peroxidase gene regulation, were numerous investigations have been carried out. A nitrogen-limited medium can trigger *lip* gene expression at the transcriptional level (Li et al. 1994), and it was confirmed that nitrogen-related compounds suppress the VA production (Fenn et al. 1981). Moreover, nitrogen nutrition also influences MnP expression as well (Pribnow et al. 1989). In another aspect, as a Mn-related enzyme, MnP activity is dependent upon manganese concentration within nitrogen-limited or carbon-limited culture; the same carbon or nitrogen resource-dependent status also found in LiP (Bonnarne et al. 1990, Gettemy et al. 1998, Pease et al. 1992). Thus, it has been suggested that availability of nutrients plus Mn(II) plays a important regulatory role for lignin-degrading enzymes. Based on promoter analysis of the *MnP* gene in *P. chrysosporium*, putative metal response elements (MREs) located within the promoter region are correlated with the activity of MnP. The existence of MREs could account for the correlation between *MnP* expression and Mn(II) (Brown et al. 1990, Brown et al. 1991). However, more research is needed to confirm the role of MREs in the regulation of lignin-degrading enzymes.

Phylogenetic studies of class II peroxidase, PODs

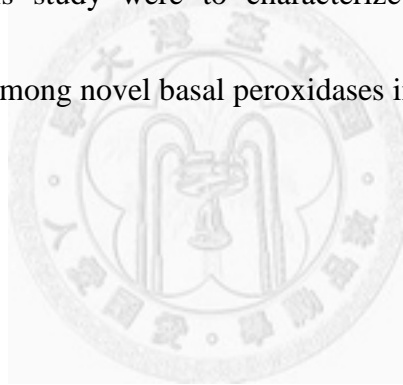
More recently, many studies focused on PODs, such as molecular characterization, enzymology, investigative tool development (e.g. transformation system), and even industrial applications, have been established (Cullen et al. 2004), however of them only few studies have focused on PODs for examining phylogenetic relationships among white and brown rot fungi. Until recently, most evolutionary research on fungi have been based on morphological data. As molecular tools have become better developed, molecular markers, especially those based on the rRNA gene cluster and mitochondrial DNA or collaborate with ecological and genetic multiple genes, have been applied for phylogenetic analyses (Bridge et al. 2005).

Preliminary phylogenetic relationship of PODs family has been assessed via nucleotide or amino acid sequence-based methods (Morgenstern et al. 2008). Analysis of phylogenetic trees derived from maximum parsimony and Bayesian inference methods, implicated that PODs clustered within a monophyletic clade. Furthermore, LiP, present in Polyporales, appears descendent from MnP. VP, whereas a multi-substrate compatible enzyme, may have evolved independently within an **single clade** (Morgenstern et al. 2008).

More recently, “Basal peroxidases” (BaP) represent a novel group peroxidases has

been found in *Postia placenta* and *A. cinnamomea*, additionally the peroxidase produced by *Coprinopsis cinerea* that was also recently regarded as BaP (Martinez et al. 2009, Morgenstern et al. 2008, Morgenstern et al. 2010). These studies revealed that BaP clade has been split from the class III plant peroxidase family earlier than the MnP and LiP lineages (Morgenstern et al. 2010). Nevertheless, more comprehensive studies are badly needed to gain a better understand of the phylogeny of BaP.

The objectives of this study were to characterize the DNA sequences and phylogenetic relationships among novel basal peroxidases in white rot fungi and brown rot fungi.



Materials and Methods

Fungal isolates, culture conditions and cultures preservation

All wood rot fungi used in this study are listed in **Table 1**. The fungi selected for investigation include five species of brown rot fungi, six species of white rot fungi, and one Ascomycetes. All fungal strains were routinely maintained on potato dextrose agar (PDA) at 25°C. Species identity was validated by PCR using ITS primers (**Table 2**). Fungal strains was achieved within cryogenic vials containing 10% glycerol mixed with 5% lactose maintained at -80°C.

Cloning of wood decay fungi partial putative *BaP* gene

Degenerate primers (**Table 2**) were designed based on the conserved regions in the amino acid sequence of class II peroxidases. The asymmetric PCR was performed using Ex Taq DNA Polymerase (Takara Bio Inc., Shiga, Japan) and the reaction mixtures composed of 2.5 µl 10x reaction buffer, 1 µl genomic DNA of target fungi, 0.5 µl 10 mM dNTP, 1 µl 20 µM of each primer (lips_1 and lipr_4), 18.7 µl ddH₂O and 2 µl Ex Taq DNA polymerase. The amplification was performed using C1000 thermal cycler (Bio-Rad Laboratories, Hercules, CA, USA) with 94°C for 10 minutes, 30 cycles at 94°C for 30 seconds, gradient annealing temperature from 42°C to 54°C for

45 seconds, 72°C for 90 seconds and followed by 72°C for 10 minutes. The PCR products were cleaned up using DNA Clean / Extraction Kit (GeneMark, Taipei, Taiwan) prepared for a second-round of PCR using nested degenerate primers. The nested PCR was carried out using 5µl aliquots of the first-round PCR product, 2.5 µl 10× reaction buffer, 0.5 µl 10 mM dNTP, 1 µl 10 µM of each primer (lips_2 and lipr_3), 14.7 µl ddH₂O, and 0.3 µl Ex *Taq* DNA polymerase in a final 25-µl reaction volume. The PCR parameters were as follows: 94°C for 3 minutes, 30 cycles at 94°C for 30 seconds, 52°C for 30 seconds, 72°C for 40 seconds, and a final extension at 72°C for 3 minutes. The amplification products were purified as previously described and cloned into pGEM-T vector system according to the instruction manual (Promega, Madison, WI, USA).

Genomic DNA extractions

Fungal mycelia (**Table 1**) harvested and ground in liquid nitrogen using 0.1 g grinding powder added to 500 µl CTAB buffer (2% CTAB, 1.4 M NaCl, 20 mM EDTA, 100 mM pH 8.0 Tris, 2% PVP-40) and 3 µl 2-mercaptoethanol preheated to 65°C. The DNA extraction mixture was incubated at 65°C for 15 minutes. An equal volume of chloroform / isoamyl alcohol (24:1) was added to each sample, and mixed gently before centrifugation at 13,200 rpm for 5 minutes. After transferring the

supernatant to a new tube, add 2/3 volume pre-chilled (-20°C) isopropanol, and incubated at -20°C for 20 minutes. The mixture was centrifuged at 10,000 g for 10 minutes to precipitate DNA, the pellet was washed twice in 75% ethanol, and air-dried for 20-30 minutes. Each DNA sample was resuspended in TE buffer (0.1 M Tris pH 8.0 and 0.01 M EDTA) treated with 0.5 µl RNase A (10 mg/ml) overnight at RT. RNAase-treated DNA was subject to Southern blot and PCR analysis.

***L. sulphureus* BaP cDNA: full-length cloning and analysis**

RNA extraction and rapid amplification of cDNA ends

RNA extraction was performed by using TRIzol reagent (Invitrogen, USA), following the protocol of the manufacturer. Mycelia (0.1-0.3 g) of *A. salmonea* and *L. sulphureus* were collected were ground to powder in liquid nitrogen, and added to 500 µl TRIzol reagent (preheated to 65°C) within tubes. The samples were gently mixed by inversion several times and then incubated at 65°C for 15 minutes, followed by centrifugation at 10,000 g for 15 minutes at 4°C. The supernatant was transferred to a new tube, and add 1/5 volume chloroform was added. The mixture was incubated at room temperature for 3-5 minutes, and subsequently centrifuged at 10,000 g for 10 minutes at 4°C. The mixture after centrifugation was separated into 3 phases; transfer the upper aqueous phase to a new tube, meanwhile carefully avoid disturbing the

interphase and lower phase. To the upper phase, 1/2 volume isopropanol containing 0.8 M sodium citrate and 1.2 M NaCl was added, and kept at 4°C for at least 30 minutes. The mixture was centrifuged at 10,000 g, 4°C for 10 minutes, discard the supernatant, washing the pellet twice with 75% ethanol and air-drying for at least 10 minutes. The RNA was suspended in DEPC-treated water or TE buffer. RNA quality was checked by denaturing gel electrophoresis. The denaturing gel contained 1/5 volume formaldehyde in 1x MOPS (20 mM MOPS pH 7.0, 5 mM sodium acetate, 1mM EDTA) and 0.8% agarose. Before loading, RNA samples were mixed with 0.5-3X volumes formaldehyde loading dye (495 µl formaldehyde loading dye composition: 60 µl 10X MOPS, 105 µl formaldehyde, 300 µl formamide, 30 µg/30 µl ethidium bromide), incubated at 70°C for 20 minutes, and immediately chilled on ice. Electrophoresis was conducted using 1X MOPS as running buffer at 100 volts for 90 minutes. The RNA sample was used for rapid amplification of cDNA ends.

Primer design

After cloning of the putative *BaP* genes from genomic DNA, a Blastx was performed based on the non-redundant protein sequence database. The translated nucleotide query sequence was aligned with other subject protein sequences. In the alignments, intron regions of putative *BaP* sequences were considered as gaps for

subject comparisons. These alignments were used to design primers for rapid amplification of cDNA ends.

Rapid amplification of cDNA ends (RACE)

Before RACE, 1 µg of total RNA of *L. sulphureus* and *A. salmonea* were treated using a Turbo DNA free kit (Ambion, Austin, TX, USA) to eliminate the DNA. The SMARTer™ RACE cDNA Amplification Kit (Clontech Inc., Palo Alto, CA, USA) and gene-specific primers (**Table 2**) were used for 3' Ends amplification. First-round PCR was conducted with 94°C for 30 seconds, 30 cycles at 94°C for 30 seconds, 68°C for 30 seconds, 72°C for 3 minutes, and 72°C for 7 minutes for final extension. Nested PCR with nested primers was performed to help reduce non-specific reactions. GSP (Table 2) was used to perform 5' Ends amplification, based on the following PCR conditions: 94°C for 3 minutes, 30 cycles at 94°C for 30 seconds, 52°C for 45 seconds, 72°C for 90 seconds, followed by 72°C for 10 minutes.

Promoter region of *MnP* gene cloning and analysis

To acquire information about the unknown region outside the 5' of *BaP* sequence, a tail-PCR strategy was used. According to the approach of Terauchi and Kahl (Terauchi et al. 2000), a series of reverse primes were designed within known

sequences of *BaP*. First-round PCR amplification was conducted in a 25- μ l reaction volumes, containing: 2.5 μ l 10X reaction buffer, 5 μ l genomic DNA, 5 μ l 1 mM dNTP, 5 μ l 10 μ M primer Ls_t5_A, 5 μ l 10 μ M 10-mer arbitrary primer, 2 μ l ddH₂O, and 0.5 μ l Ex Taq DNA polymerase. The detailed PCR parameters and conditions are shown in **Table3**. For second round PCR amplification, 1 μ l 1/50 dilution of first-round PCR product was used as template. Second-round PCR-mixture composition was the same as the first round, except that primer Ls_t5_A was replaced with Ls_t5_B. Third-round PCR mixtures contained 5 μ l of 1/10 dilution of second-round PCR product as template, 2.5 μ l 10X reaction buffer, 5 μ l 10 μ M 10-mer arbitrary primer, 5 μ l 1 mM dNTP, 2 μ l ddH₂O, and 0.5 μ l Ex Taq DNA polymerase. Separate amplifications were performed using 5 μ l gene-specific primer 10 μ M Ls_t5_C1-C3, independently.

The putative transcription factor binding sites (TFBS) were systematically analyzed using Genomatix MatInspector (<http://www.genomatix.de/matinspector.html>, Genomatix Software, Munich, Germany) (Cartharius et al. 2005).

Gene copy number determination: Southern blot analysis

Isolation of *L. sulphureus* genomic DNA was conducted as described previously. DNA was digested with *Pst*I, *Hind*III, *Afl*III / *Pst*I, *Eco*RV / *Hind*III and *Pst*I / *Eco*RV

(New England Biolabs, Beverly, MA, USA) and separated on 0.8% (w/v) agarose gel. Electrophoresis was conducted at 50 Volts for 6 hours. Before DNA transfer, the gel was first incubated in 0.25 N HCl at room temperature for 30 minutes, and rinsed twice with ddH₂O. The gel was immersed in denaturing solution (1.5 M NaCl, 0.5 N NaOH) for 20 minutes and repeated once, before incubating in neutralization solution (3 M NaCl, 0.5 M Tris base, 70.2 g Tris·HCl per liter) for 30 minutes. The capillary transfer apparatus was prepared using 20 X SSC (3 M NaCl, 0.3 M Na₃Citrate, 1 M HCl, pH 7.0) as transfer buffer, and HybondTM-N+ nylon membrane (GE healthcare Bioscience, Piscataway, NJ, USA) as the blot membrane. After transfer process was conducted overnight, the membrane was rinsed with 2X SSC for 5 minutes, and DNA on the membrane was cross-linked with an XL-1000 UV crosslinker (Spectronics, Westbury, NY, USA) using 120 mJ / cm². Hybridization was performed using an LsaP probe generated by PCR with primers A0427_forward and A0902_R. To label the probe, Roche DIG DNA labeling kit (Roche Molecular Biochemicals, Mannheim, Germany) Dig-labelled dNTP was used instead of dNTPs during PCR amplification. The membrane was prehybridized with hybridization buffer (50% deionized formamide [w/v], 0.25 M NaH₂PO₄, 50 mM NaCl, 1 mM EDTA, 0.005% sperm DNA [w/v], 3.5% SDS [w/v]) for 5 hours. Hybridization was conducted in a rotatory glass tube overnight at 55°C, then the membrane was washed in 2X SSC / 0.1% SDS at

room temperature for 15 minutes; re-washed at 62°C in 25 mM NaH₂PO₄ / 1 mM EDTA / 0.1% SDS and 25 mM NaH₂PO₄ / 1 mM EDTA / 1% SDS, respectively. After stringency washing, the membrane was equilibrated with 0.3% Tween 20 maleate buffer (0.1 M maleic acid, 0.15 M NaCl pH 7.5) and incubated with blocking solution (1-2% blocking reagent; Roche Molecular Biochemicals) for 30 minutes. The Dig-labeled probe was conjugated with Anti-Digoxigenin-AP Fab fragments (Roche Molecular Biochemicals) and the signal detected on Super RX X-ray film (Fujifilm, Tokyo, Japan) via the presence of chemiluminescent substrate CDP-Star[®] Nucleic Acid Chemiluminescence Reagent (PerkinElmer, Boston, MA, USA).

Induction for *MnP* gene expression and analysis

Culture conditions of *L. sulphureus*

First, *L. sulphureus* was grown in PDA Petri plates at 25°C for 7 days, and ground mycelium collected was subcultured in PDB liquid medium at 25°C for 7 days at 150 rpm. The yielded mycelia were washed twice with ddH₂O, then transferred to a basal medium that developed for *P. chrysosporium* with slight modification (Kirk et al. 1978). The basal medium is comprised of 0.2 g KH₂PO₄, 0.05 g MgSO₄·7H₂O, 0.01 g CaCl₂, 0.001 g thiamine, 20 g glucose (carbon source), 2.2 g ammonium tartrate (12 mM), 9 g sodium succinate (20 mM) pH 4.5, 0.1 ml mineral solution, which consists of

1.5 g nitrilotriacetate, 3 g $\text{MgSO}_4 \cdot 7\text{H}_2\text{O}$, 1 g NaCl, 100 mg $\text{FeSO}_4 \cdot 7\text{H}_2\text{O}$, 100 mg CoSO_4 , 82 mg CaCl_2 , 100 mg ZnSO_4 , 10 mg $\text{CuSO}_4 \cdot 5\text{H}_2\text{O}$, 10 mg $\text{AlK}(\text{SO}_4)_2$, 10 mg H_3BO_3 , 10 mg NaMoO_4 and 0.05 ml vitamin solution (2 mg biotin, 5 mg riboflavin, 5 mg pyridoxine · HCl, 10 mg cyanocobalamine, 0.1 mg nicotinic acid, 5 mg DL-calcium pantothenate, 5 mg ρ -aminobenzoic acid, and 5 mg thioctic acid per 1 H_2O). After culture for 24 hours, different concentrations of MnSO_4 and veratryl alcohol (3,4-dimethoxybenzyl alcohol, VA) were added for different induction conditions. For the low Mn ion sample, 18 μM Mn final concentration was used; for high Mn ion sample, 180 μM Mn was used; for the veratryl alcohol-treated sample, 0.5 mM veratryl alcohol was used. All solutions and media were filtered through 0.22 μm -mipore filter before use.

Extraction of RNA under different incubation conditions and time course

After induction with different concentrations of MnSO_4 and VA, mycelia were harvested after incubation for 24, 48, and 72-hour, respectively. The mycelia was filtered using a Büchner funnel with qualitative 70-mm filter (Whatman International, Ltd., Maidstone, UK), and connected to Büchner flask by a neoprene adapter and a vacuum pump. RNA extraction was performed using the Plant Total RNA Extraction Mini kit (Viogene, Taipei, Taiwan), following the protocol provided by the

manufacturer. DNA was eliminated and denaturing gel electrophoresis of RNA was carried out as mentioned previously. All RNA samples were stocked at -20°C until further analysis.

Reverse transcriptase-polymerase chain reaction (RT-PCR)

RT-PCR was conducted with superscript II reverse transcriptase (Invitrogen, Life Technologies, Inc., Rockville, MD, USA). In each reaction mixture, 1 µg RNA of *L. sulphureus*, 1 µl 10 mM dNTP mix, 1 µl 10 µM Oligo-dT₁₅ were added to DEPC-treated ddH₂O for a total reaction mixture volume of 12 µl, and incubated at 65°C for 5 minutes. After chilling on ice, added 4 µl 5X first-strand buffer and 2 µl 0.1 M DTT to the mixture, incubated at 42°C for 2 minutes. Next, add 1 µl (200 U) superscript II reverse transcriptase, and RT was executed at 42°C for 50 minutes, and then terminated at 72°C for 15 minutes. An RT-minus control was also conducted to verify the absence of contaminated DNA. After RT-PCR, cDNA products were stored at -20°C until further use.

Real-time quantitative PCR (qPCR) analysis

To assess differential expression of *LsBaP* affected by different induction factors (VA, high Mn, low Mn), the housekeeping gene glyceraldehyde-3-phosphate

dehydrogenase (*gapdh*) was used as an internal control using qGA_F and qGA_R primers. For analysis of *BaP* expression Real-time PCR was conducted using the *BaP*-specific primers 1018F and 1018R. In each experiment, biological triplicates were performed using the StepOnePlus™ Real-Time PCR System (Applied Biosystems, Inc., FosterCity, CA) with Power SYBR® Green PCR Master Mix (Applied Biosystems). Each reaction mix (5 µl 2X master mix, 1 µl 1/10 diluted cDNA preparation, 0.2 µl 10 µM primer C, 0.2 µl 10 µM primer D, and 3.6 µl ddH₂O) was loaded into the MicroAmp® Fast 8-Tube Strip (Applied Biosystems), 0.1 ml covered with MicroAmp® Optical 8-Cap Strip (Applied Biosystems). Conditions for qPCR were as follows: 95°C for 10 minutes, followed by 40 cycles at 95°C for 15 seconds, 60°C for 1 minute. The specificity of primers was confirmed by melting-curve analysis. Data collection and analysis was performed using StepOne™ software v2.2.2 (Applied Biosystems) and Microsoft Office Excel 2010 (Microsoft Corp., Redmond, WA, USA).

Modeling the 3-D molecular structure of basal peroxidase

Protein 3-D molecular homology modeling with deduced *LsBaP* amino acid sequence was implemented using the SWISS-MODEL workspace (<http://swissmodel.expasy.org>), which is linked to protein data bank, RCSB PDB

(<http://www.rcsb.org/pdb/home/home.do>). Automated mode was chosen as the processing mode, the query sequence was aligned with PDB sequences, and 3-D molecular model prediction conducted automatically on the server. Further analysis and comparison with versatile peroxidase and basal peroxidase were performed using PyMOL software (DeLano 2002) and 3D molecule viewer (Informax Inc., Invitrogen, Carlsbad, CA, USA).

BaP sequences alignment and phylogenetic tree construction

Sequences collection and alignment

In addition to partially deduced amino acid sequences of the cloned putative peroxidases, additional class II peroxidase sequences, primarily from a modified data set from Morgenstern et al.(2010), were in cooperated for comparison. **Table 4** lists all sequences and reference that were used in this analysis.

Multiple sequence alignments were performed using ClustalX2 (Larkin et al. 2007) with the following parameters: gap opening penalty = 10, gap extension penalty = 0.01, score matrix = Gonnet250; and pairwise alignment parameters were as follows: gap opening penalty = 10, gap extension penalty = 0.1, score matrix = Gonnet250. The final alignments were adjusted by visual check. Due to length disparities among the

aligned sequences, all sequences beyond the alignment region were deleted. The alignment arrangement was executed by MEGA 5 (Tamura et al. 2011).

Whole-sequence alignments were subject to Maximum likelihood tree analysis.

Another selected dataset produced from the same alignment procedure was also subject to analysis by neighbor-joining and Bayesian inference methods.

Phylogenetic tree construction by Maximum likelihood (ML) method

Prior to tree construction, the WAG substitution matrix was determined to be the most suitable for analysis, based on the model test of MEGA 5. The ML tree was constructed by RAxML using a rapid bootstrap algorithm (Stamatakis et al. 2008) and bootstrapping was automatically limited by RaxML default settings .

Phylogenetic tree construction by Neighbor-joining (NJ) method

NJ tree based on a minimum evolution concept was also constructed using MEGA 5 with a JTT substitution model, and phylogeny analysis was performed with 1000 bootstrap replications. All gaps in the sequences were treated by complete deletion.

Phylogenetic tree construction by Bayesian inference method

According to Bayesian theory, the following formula is used to describe the relationship between probabilities of two events and their conditional probabilities:

$$P(A|B) = \frac{P(B|A)P(A)}{P(B)}$$

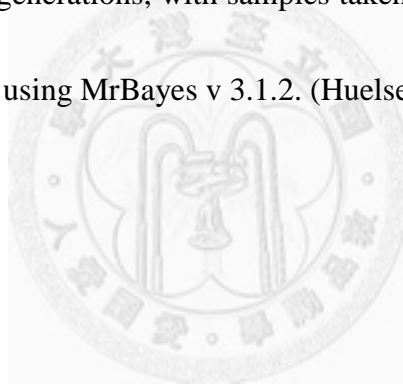
$P(A|B)$, which refers to the posterior probability of A, is the probability of P(A) as B occurs. In relation to phylogenetic tree construction, basically the Bayesian inference (BI) method is similar to the Maximum likelihood method except for the prior distribution which is based on various given trees. Through MCMC runs, the initial chain is defined based on a particular substitution model, rate variation... etc. According to the Bayesian theorem, the posterior probability (Pr) is defined as follows:

$$\Pr(\text{Tree}|\text{Data}) = \frac{\Pr(\text{Data}|\text{Tree})\Pr(\text{Tree})}{\Pr(\text{Data})}$$

A new tree is generated and given a ratio of probabilities from a previous state.

$$R = \frac{\Pr(\text{Tree}_j)\Pr(\text{Data}|\text{Tree}_j)}{\Pr(\text{Tree}_i)\Pr(\text{Data}|\text{Tree}_i)}$$

Simultaneously, the generated tree with R value higher than 1 could be retained or another tree would regenerate. After many generations, the state becomes stabilized and approximates the real condition. Meanwhile, several chains typically containing at least one cold chain are also incorporated in the run avoid suboptimal fixation of the chains fixing. The swapping would occur if chains got stuck in distributions of relative lower probability (Hall 2007). The consensus tree optimization was performed by Markov chain Monte Carlo (MCMC) chains with 4 chains, including 1 cold and 3 heated chains for 1 million generations, with samples taken every 100 generations. All approaches were performed using MrBayes v 3.1.2. (Huelsenbeck et al. 2001).



Results

Cloning and characterization of putative PODs genes

According to previous studies, none of class II fungal secretory peroxidase genes have been cloned and characterized except for ligninolytic peroxidase of *A. cinnamomea* (*AcLnP*) (Huang et al. 2009). That result from *A. cinnamomea* might imply that PODs orthologs exist in genomes of brown rot fungi. Several amplicons derived from different brown rot fungi were amplified using degenerate primers and varied PCR conditions (**Fig. 1**). Sequences of PCR-product were identified by blastx, indicating these partial cDNA fragments were homologous to *AcLnP*, and they also have higher similarity to *MnP* rather than *LiP* and *VP*. Besides, the fragments were identified as PODs as the existence of two characteristic features of PODs: heme-binding site and calcium-binding site within the fragments.

Putative class II peroxidase gene sequences from the brown rot fungi *L. sulphureus* and *A. salmonea* were similar to each other and being selected for further analysis. Full-length cDNAs from these two fungi were obtained by rapid amplification of cDNA ends (RACE) (**Fig. 4**). After RACE, new primers to amplify complete sequences of putative *LsBaP* and *AsBaP* genes were designed and PCR was performed.

The amplicons harbored full-length cDNAs of 1,278 bp and 1,363 bp for *LsBaP* and *AsBaP*, respectively. Based on in silico analysis using Spidey (<http://www.ncbi.nlm.nih.gov/spidey>) the exon/introns sites were mapped. The resulting map (**Fig. 4**) shows that the full-length of *LsBaP* gene is 1,950 bp, which contains 10 introns and 11 exons. Furthermore, results from the Southern Blot indicated that the *L. sulphureus* genome contains only a single copy of *LsBaP* (**Fig. 4**).

The deduced amino acid sequences of *LsBaP* are shown in **Fig. 5**. The full-length cDNA sequences indicating that *LsBaP* encodes a protein comprises 340 amino acids, with the characteristic features of a class II peroxidase, including a heme-binding site and calcium-binding sites. Cleavage of the 20-amino-acid signal peptide congenerates the mature protein.

Comparison of exon/intron distribution in *LsBaP* and *AsBaP* with secretory peroxidases from Basidiomycetes fungi

Compared with *LsBaP* and *AsBaP*, exon/intron distribution within basal peroxidase genes from *Postia placenta* Pp 44056 (Martinez et al. 2009), *Coprinus cinerea* peroxidase *CiP* (Baunsgaard et al. 1993, Stajich et al. 2010), *Phanerochaete*

chryso sporium basal peroxidase Pch1 6250 (Martinez et al. 2004), *Lentinus edodes* manganese peroxidase *LeMnP2* (Sakamoto et al. 2009), *Phanerochaete chryso sporium* lignin peroxidase *PcLiP* (Naidu et al. 1990), *Arthromyces ramosus* peroxidase *ArP* (Sawai-Hatanaka et al. 1995), and *Phanerochaete chryso sporium* lignin peroxidase H8 *PcLiP H8* (Andrawis et al. 1989) were subject to the analysis. In contrast to many lignin peroxidase genes with a typical exon/intron pattern, unusually small exons were found on or in close proximity to the 5' terminal, and relatively larger exons were located on 3' terminal of *AsBaP*, *LsBaP*, *CiP*, Pp 44056, Pch1 6250 and *LeMnP2*. Exon distribution appeared to be remarkably conserved among *AsBaP*, *LsBaP*, and *CiP*. Furthermore, introns of *Pclip* and *Pclip H8* generally followed the GT-AG rule, except for the intron located at or near to the 5' terminal of *AsbaP*, *LsbaP*, *CiP*, and Pp 44056 (**Fig. 6**).

Promoter analysis of *LsBaP*

After tail-PCR (Terauchi et al. 2000), about 3,000 bp of the 5'-flanking region of *LsBaP* was amplified (**Fig. 7**). Analysis of *LsBaP* 5' flanking region revealed the presence of two metal regulatory element factors, two yeast heat-shock factors, RNA polymerase II transcription factor II B, and three carbon source-responsive elements (**Figs. 5 and 7**). The putative TATA box was identified 46 bp upstream from the

transcription start site, followed by core promoter motif ten elements at 10 bp downstream.

Comparison of *LsBaP* expression under different culture conditions

Real-time quantitative RT-PCR (qPCR) was performed to measure transcript abundance of *LsBaP*. The RT-PCR and melting curve test taken place ensured the validity of this gene expression study. After induction with 180 μ M Mn ion, *LsBaP* transcripts were increased 3.5-fold relative to the non-induced control on day 1; however, transcript induction was not noticeable at day 2 and thereafter. With the VA treatment, the transcript level showed a slight down-regulation. Inexplicably, transcription level of the control, which was cultured in manganese-free medium, appeared to increase slightly over time, compared to cultures treated with either VA or MnSO₄. (Fig. 8)

Modeling the 3-D molecular structure of basal peroxidase

Alignments and analysis of the queried sequence and other database sequences indicated that *Coprinus cinereus* peroxidase (PDB ID: 1LY8) (Houborg et al. 2003) was the most appropriate basis for homology modeling . The amino acid sequences start from 20 - 340 were used for modeling, because amino acid sequences 1 - 20 could

constitute a signal peptide region that undergoes alternative splicing during translation (Fig. 5). LsBaP and template (CiP) exhibit 47.37% sequence identity and 0.00e-1 E-value. Several statistic potential parameters were used to estimate the reliabilities of modeling: c_{β} interaction energy, all-atom pairwise energy, solvation energy, and torsion angle energy. These factors contribute to QMEAN4 score calculation. The QMEAN score was normalized to QMEAN Z-score through reference structures of similar size with the query (+/- 10%) determined by X-ray crystallography. The QMEAN 4 raw score and QMEAN Z-score for our modeling were 0.7 and -1.25, respectively.

Comparison between protein structure of LsBaP and VP

Certain key amino acid residues of LiP and MnP, such as Trp171 in LiP or Glu35, Glu39 and Asp79 in MnP1, attributes to VA- and manganese-binding sites, respectively, in *P. chrysosporium* also in versatile peroxidase of *P. eryngii*. As shown in Fig. 10, the search for residues corresponding to the VA-binding site in basal peroxidase from *L. sulphureus* suggest that it is a typical heme-binding site with distal and proximal histidines (His48 and His176) within the core of whole protein, as was predicted. However, the mediator VA-related residue tryptophans, which should correspond with one side of the heme-binding site, do not appear in the appropriate

dimensional location for BaP. Moreover, the Mn-binding pocket, composed of Glu36, Glu40 and Asp175 in VP also appears atypical in BaP, which contains three distinctive amino acid substitutions (Glu20, Gly32 and Asn120) in the approximate placement of the essential amino acids.

Phylogenetic analysis usingn method of Maximum likelihood, Neighboring-joining and Bayesian inference

The phylogenetic tree was generated by Maximum likelihood analysis of basal peroxidase genes from 153 fungal taxa, including basidiomycetes white-rot fungi, brown-rot fungi, and even species of Ascomycota. The topology of the phylogenetic tree shows that all taxa are distinctly clustered within a single clade, with the class II peroxidase family at the base (**Fig. 11**). Phylogenetically, the CiP and peroxidase from *Coprinellus disseminatus* appear close to the BaP cluster. Interestingly, Phchr1 6250 and PP (AAU 82081) from *P. chrysosporium*, which are both considered basal peroxidases, are contained within LiP family subclade. Overall, this phylogenetic analysis strongly indicates that basal peroxidase is paraphyletic with respect to MnP, VP, and LiP.

In an attempt to increase support values for phylogenetic analysis, the neighbor-joining method was used to construct another phylogenetic tree based on a smaller dataset that contained 86 taxa. However, the resulting bootstrap values for basal branches of the NJ tree were still less than desirable (**Fig. 12**). Most noteworthy is that trees derived from the ML and NJ trees exhibited similar topologies; and NJ analyses placed Phchr1_6250 and PP from *P. chrysosporium* close to the BaP clade, in congruence with result of Bayesian analysis and previous studies (Morgenstern et al. 2010). Furthermore, the phylogenetic tree resulting from Bayesian analysis also exhibits topology similar to the ML and NJ trees (**Fig. 13**). Although a few polytomies occurs near some terminal nodes, the key basal nodes are supported more strongly by posterior probability values (> 0.9), compared with the ML and NJ trees. These analyses all came up to a similar conclusion: basal peroxidase is a specific type of protein that shows similarities with CiP, but is distinct from other class II peroxidases.

Discussion

Potential ligninolytic activities in brown rot fungi

Secretory fungal peroxidases have been regarded as the most important enzymes in the lignin degrading process due to their higher redox potential compared to other oxidative enzymes. Several types of peroxidases have been identified and cloned from various white-rot fungi, especially in *P. chrysosporium*, which is a model system for class II peroxidase. Based on the discoloration test, low laccase activity was detected in the brown rot fungus *Oligoporus fragalis* and Mn-dependent peroxidase activity was found in another brown rot fungus *Piptoporus betulinus* (Szklarz et al. 1989, Worrall et al. 1997). However, gene sequence information is needed to confirm the existence of class II peroxidases in brown rot fungi. The recent isolation of a novel ligninolytic peroxidase gene (LnP) from *A. cinnamomea*, a medicinal fungus in Taiwan, provides an example of lignin degradation related peroxidase gene cloning and characterization. The function of *A. cinnamomea* LnP was confirmed with on various dye discoloration tests (e.g., Bromophenol blue, 2,6-dimethoxyphenol and guaiacol) and heterologous expression (Huang et al. 2009). In contrast to traditional conceptuals, the results implicated the existence of class II peroxidase in brown rot fungi and revived further study.

Basal peroxidase of *L. sulphureus* represents a class II peroxidase based on sequence characteristics

In our investigation, we chose a fast-growing Basidiomycota *L. sulphureus* (Basidiomycota, Polyporaceae) as a model poroid organism, which was characterized with wide host range and capable to colonize to both conifers and hardwoods. Our PCR results further revealed the existence of that LnP-like genes in several brown rot fungi (**Fig. 1**). Furthermore, the deduced amino acid sequences showed higher similarity to LnP of *A. cinnamomea* than other types peroxidases by blastx. The nucleotide sequences of the amplicons were highly conserved across immense member of taxa, which further indicates that these genes derived from different species are homologous. To further establish the identity of putative LiPs, the blastx approach was combined with the conserved domain database (CDD) to analyze the class II peroxidase (**Fig. 3**). Besides the heme-binding site, a conserved feature among most peroxidases, additional crucial factor for extracellular peroxidase is the structure calcium which stabilizes enzyme structure under thermal pressure (Sutherland et al. 1996). Actually via the CDD-based approach the existence of Ca²⁺-binding sites within LiPs fragments was demonstrated. Based on these results disclosed, the putative LiPs should be classified as class II peroxidases.

Expression of LsLnP is induced by MnSO_4 , but much less than typical manganese peroxidase.

According to previous studies on *P. chrysosporium*, many factors, such as the limitation of carbon or nitrogen source, can influence gene expression and enzyme activity of class II peroxidases (Faison et al. 1985, Jeffries et al. 1981, Keyser et al. 1978, Pease et al. 1992). In addition, some trace elements, i.e. calcium and manganese, can also maneuver the ligninase activity and gene expression (Gettemy et al. 1998, Jeffries et al. 1981). The expression of three *mnp* isogenes in the genome of the *P. chrysosporium* model system is regulated by manganese under conditions of nitrogen deficiency at the transcriptional level (Brown et al. 1990, Brown et al. 1991). Due to the high similarity to MnP shown in the blastx result, we suggested that the putative ligninolytic peroxidase gene of *L. sulphureus* (hereafter referred to as *pMnP*) was an orthologue of *MnP* in *P. chrysosporium*. The assumption was further verified by real-time RT-PCR of *pmnp* expression enhanced by manganese. *pmnp* expression actually could be triggered by 180 μM MgSO_4 , though no response at 18 μM MgSO_4 and unexpectedly VA down regulated the expression slightly (**Figure 8**). *P. chrysosporium* and *Fomitiporia mediterranea* showed relatively high levels expression of *mnp* (Morgenstern et al. 2010). The expression of *pmnp* of *L. sulphureus* was notably lower compared to *mnp* of *P. chrysosporium* and *F. mediterranea* when activated by MnSO_4 .

These results perhaps may attribute to suboptimal conditions for *pmnp* expression, or regulatory mechanisms of *pmnp* are different from typical *mnp*. Thus, it's essential to understand that relationship between manganese and *mnp*.

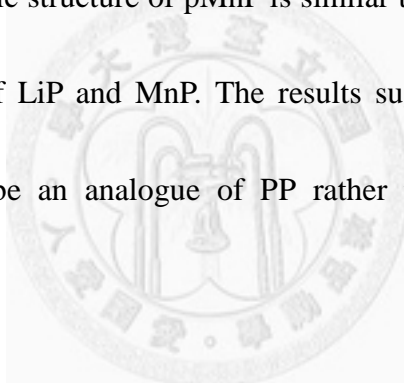
Previous studies on *P. chrysosporium* showed that, paired MREs located within the promoter region of *MnP* (Godfrey et al. 1990, Mayfield et al. 1994), which correlated with the high expression of *mnp1* and *mnp2* (Cullen et al. 2004, Gettemy et al. 1998). Analysis of the *pmnp* promoter region of *L. sulphureus* in this study also revealed the existence of two unpaired putative MREs (**Fig. 4**). Interestingly, the *mnp3*, an isogene within the *mnp* family of *P. chrysosporium*, also harbored two unpaired MREs in the promoter region, but not strongly regulated by Mn (Alic et al. 1997, Gettemy et al. 1998). The homologues of the unpaired MREs in *mnp3* and *pmnp* may account for relatively low up regulation of *pmnp* by Mn, compared with *mnp1* and *mnp2*. Additional, in subsequent mutation study by disruption *mnp1* and an *egfp* marker to examine the function of MRE sequences, promoter analysis of *P. chrysosporium mnp1* suggested that a novel 33-bp sequence, a highly homologous sequence among genes encoding *mnp* isozymes, could be a critical induction factor in response to Mn. The results suggested that paired MREs may not play a major role in *mnp1* regulation (Ma et al. 2004). Likewise, up regulation of *mnp2* gene by Mn(II) in

Trametes versicolor can occur without MREs (Johansson et al. 2002). Conclusion came up from these investigation totally imply the necessity to clarify the role of MREs in the *mnp* regulatory mechanism and the attempt in another angle was applied to intensify that *pmnp* of *L. sulphureus* is actually a member of the class II peroxidase family.

Virtual protein structure modeling analysis of pMnP

Since it has a heme- and a calcium binding site within the deduced amino acid sequence of pMnP (**Fig. 3**); an alternative homologous modeling approaches was enforced by using putative crystallographic modeling analysis using LiP and MnP from *P. chrysosporium* and *Pleurotus eryngii* as a modeling system. (Choinowski et al. 1999, Poulos et al. 1993, Ruiz-Dueñas et al. 1999, Sundaramoorthy et al. 1994). Using Swiss-Model structure modeling, the modeling template can be selected based on an optimization process for protein, gapped blast. The program selected the *Coprinus cinereus* peroxidase (CiP, PDB id:1LY8) (Houborg et al. 2003) as the optimal template. To further characterization of pMnP, the 3-D structure of pMnP was superimposed with versatile peroxidase from *Pleurotus eryngii* (PDB id: 3FM1, to be published). This comparison between VP and pMnP was under the parameter in consideration for the duality of versatile peroxidase, which contains both Mn- and VA-binding sites. Similar

comparison with VP from *P. eryngii* and peroxidase from *P. placenta* (PP) (Martinez et al. 2009), heme cofactor of pMnP is located internally in typical fashion as other class II peroxidases; whereas residues correlated to the Mn-binding site and VA-binding site are not typical. In the structure of VP from *P. eryngii*, the Mn-binding site consists of three residues, Glu36, Glu40 and Asp175, however, in the case of pMnP of *L. sulphureus* the residues were substituted by Glu20, Gly32 and Trp18 (**Fig. 10**). Moreover, the VA pocket found in VP is not present in pMnP. The configuration suggests that crystallographic structure of pMnP is similar to PP, because both lack the notably catalytic activity of LiP and MnP. The results suggest that pMnP, hereafter referred to as BaP, may be an analogue of PP rather than a typical ligninolytic peroxidase.



Ligninolytic activities beyond white rot fungi

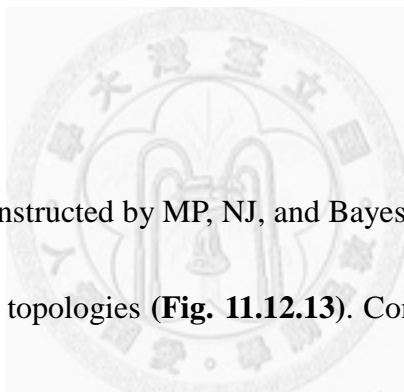
To further clarify the possible evolutionary route of BaP, three different phylogenetic analyses were performed. More recently, a systematic and comprehensive analysis of wood decay mechanisms, substrate preference, host range and mating types carried out by Hibbett (2001). The study indicated that brown rot fungi exclusively colonized and degraded conifer wood, in mating system, heterothalics evolved towards homothalics by repeatedly gaining and losing mating genes (Hibbett et al. 2001).

Moreover, they hypothesized that brown rot fungi were evolved repeatedly from white rot fungi, may have lost but retained some genes related to wood degradation (Hibbett et al. 2001). Currently, a few ligninolytic activity within brown rot fungi has been demonstrated in a few Basidiomycetes as well as Ascomycetes (Enoki et al. 1988). More recently, evidence derived from molecular study has indicated the limited lignin modification capability, an essential trait for brown rot Basidiomycetes to access the integrated cellulose or hemicellulose in the wood as exemplified in *A. cinnamomea*, *G. trabeum*, *P. placenta* (Dey et al. 1994, Enoki et al. 1988, Huang et al. 2009, Niemenmaa et al. 2008).

Phylogenetic analysis: Likelihood of BaP as a novel class II peroxidase

However, our preliminary study implicated an array of brown rot Basidiomycetes and Ascomycetes may employ this attribute to sustain on substrate for survival. It is meaningful, in terms of nutrient recycling and ecology. Results from our sequence alignments, qPCR, and putative protein structure analysis all indicate that BaP class II peroxidase is quite distinct from previously characterized fungal peroxidases, ligninase. Furthermore, outcome of the phylogenetic analysis supports the assumption that BaP is a monophyletic gene family within the fungal peroxidase genes, and particularly noteworthy that BaP not only occurs in many taxa of Basidiomycota but

also in some wood-inhabiting Ascomycota (**Fig. 11**). Furthermore, result also indicated *Coprinus cinerea* peroxidase (CiP), the closest peroxidase relative of BaP also juxtaposed at the base of the class II peroxidase clade. Nevertheless, CiP has the capacity to oxidize some phenol or dyes (Kjalke et al. 1992), which could account for the positive decoloration assays shown in *A. cinnamomea* and other brown rot fungi (Huang 2008). On perspective, to precisely define the function of ligninolytic peroxidase, via gene insertion or disruption to gain or loss the function of this BaP in brown rot fungi is needed.



The consensus trees constructed by MP, NJ, and Bayesian analyses showed highly congruency in terms of tree topologies (**Fig. 11.12.13**). Comparison between BaP part of gene tree and evolutionary tree of Basidiomycetes (**Appx Fig. 2**) (Hibbett 2006) reveal no complete consistency no matter for ML, NJ or BI tree. However, in the BaP part of whole peroxidase gene tree express different topologies among ML, NJ and BI tree. It might be caused by deficient sequence information or inappropriate evolutionary marker gene usage for *bap*. Similar result derived from higher level of class II peroxidase gene tree in previous report. Location of Polyporales on the latest lineage of class II peroxidase gene tree instead of Agaricales in the evolutionary tree (Morgenstern et al. 2008, Morgenstern et al. 2010) could be regard as that evolution of

PODs is not entirely parallel with species themselves. The latest generated organismal phylogeny (chronogram) using BEAST shows better linkage between PODs tree and evolutionary tree (Floudas et al. 2012).

In agreement with previous studies, our phylogenetic analyses indicate that fungal secretory peroxidases, except BaPs, only occur within Basidiomycetes that evolved after the separation of Basidiomycetes and Ascomycetes. (Morgenstern et al. 2008). Notably, BaPs exist in diverse families of Gloeophyllales, Polyporales, Hymenochaetales, Agaricales, and even Ophiostomataceae (Ascomycete). Does BaP actually normally exist across the phylum of Basidiomycota and Ascomycota is an intriguing puzzle to be resolved. Nevertheless, based on the phylogenetic topology BaP appears to have evolved much earlier than other class II peroxidases.

Morgenstern (2010) suggested that the class II peroxidase family, LiPs evolved from VPs or MnPs by gene loss events. Accordingly, the member in Polyporales, no matter white rot or brown rot, may possess basal peroxidases. Because BaP may be found in Ascomycetes, a polyphyletic assemblage that appears evolutionarily older than Agaricomycetes, implications are that BaPs is perhaps comprised within a larger group that extends beyond what is currently known. BaPs is likely the ancestor of

DOPs and have no capacity of lignin degradation due to lack of Mn-binding site and Trp171. It implies that lignin degradation mechanism is a unique ability belongs to some Basidiomycetes. Furthermore, the diversification of white rot and brown rot is caused by series of contractions in PODs (Floudas et al. 2012) except for BaP.

Although the proximal node the bootstrap and posterior probability values for the branches of the phylogenetic trees are not high, all three phylogenetic analyses are congruent with previous studies (Martinez et al. 2009, Morgenstern et al. 2008, Morgenstern et al. 2010). A focus on relationships among BaPs and LiPs, MnPs, VPs, demonstrates that LiPs and MnPs are both derived from BaPs (Martinez et al. 2009). Our result further boosted that BaPs present in Basidiomycetes and Ascomycetes also implicated that BaPs in Ascomycetes or Basidiomycetes are evolutionary predecessors of LiPs and MnPs; also the speciation, gene duplication, and ligninase gene loss events (Floudas et al. 2012, Martinez et al. 2009) appear to have occurred before the evolutionary split of brown rot and white rot fungi; the evolution of MnPs and LiPs appears to have occurred independently from BaPs.

Reference

- Abbasi, T. and Abbasi, S. 2010. Biomass energy and the environmental impacts associated with its production and utilization. *Renewable and Sustainable Energy Reviews* 14:919-937.
- Alic, M., Akileswaran, L., and Gold, M.H. 1997. Characterization of the gene encoding manganese peroxidase isozyme 3 from *Phanerochaete chrysosporium* 1. *Biochim. Biophys. Acta, Protein Struct. Mol. Enzymol.* 1338:1-7.
- Andrawis, A., Pease, E.A., Kuan, I., Holzbaur, E., and Tien, M. 1989. Characterization of two lignin peroxidase clones from *Phanerochaete chrysosporium*. *Biochem. Biophys. Res. Commun.* 162:673-680.
- Asada, Y., Watanabe, A., Irie, T., Nakayama, T., and Kuwahara, M. 1995. Structures of genomic and complementary DNAs coding for *Pleurotus ostreatus* manganese (II) peroxidase. *Biochim. Biophys. Acta, Protein Struct. Mol. Enzymol.* 1251:205-209.
- Baunsgaard, L., DALBØGE, H., Houen, G., RASMUSSEN, E.M., and Welinder, K.G. 1993. Amino acid sequence of *Coprinus macrorhizus* peroxidase and cDNA sequence encoding *Coprinus cinereus* peroxidase. *Eur. J. Biochem.* 213:605-611.
- Black, A.K. and Reddy, C. 1991. Cloning and characterization of a lignin peroxidase gene from the white-rot fungus *Trametes versicolor*. *Biochem. Biophys. Res. Commun.* 179:428-435.
- Blodig, W., Smith, A.T., Winterhalter, K., and Piontek, K. 1999. Evidence from spin-trapping for a transient radical on tryptophan residue 171 of lignin peroxidase. *Arch. Biochem. Biophys.* 370:86-92.

- Bonnarme, P. and Jeffries, T.W. 1990. Mn (II) regulation of lignin peroxidases and manganese-dependent peroxidases from lignin-degrading white rot fungi. *Appl. Environ. Microbiol.* 56:210.
- Bridge, P., Spooner, B., and Roberts, P. 2005. The impact of molecular data in fungal systematics. *Adv. Bot. Res.* 42:33-67.
- Brown, J., Glenn, J., and Gold, M. 1990. Manganese regulates expression of manganese peroxidase by *Phanerochaete chrysosporium*. *J. Bacteriol.* 172:3125.
- Brown, J.A., Alic, M., and Gold, M.H. 1991. Manganese peroxidase gene transcription in *Phanerochaete chrysosporium*: activation by manganese. *J. Bacteriol.* 173:4101.
- Camarero, S., Sarkar, S., Ruiz-Dueñas, F.J., Martínez, M.J., and Martínez, Á.T. 1999. Description of a versatile peroxidase involved in the natural degradation of lignin that has both manganese peroxidase and lignin peroxidase substrate interaction sites. *J. Biol. Chem.* 274:10324-10330.
- Cancel, A.M., Orth, A., and Tien, M. 1993. Lignin and veratryl alcohol are not inducers of the ligninolytic system of *Phanerochaete chrysosporium*. *Appl. Environ. Microbiol.* 59:2909-2913.
- Cartharius, K., Frech, K., Grote, K., Klocke, B., Haltmeier, M., Klingenhoff, A., Frisch, M., Bayerlein, M., and Werner, T. 2005. MatInspector and beyond: promoter analysis based on transcription factor binding sites. *Bioinformatics* 21:2933-2942.
- Choinowski, T., Blodig, W., Winterhalter, K.H., and Piontek, K. 1999. The crystal structure of lignin peroxidase at 1.70 resolution reveals a hydroxy group on the C β of tryptophan 171: A novel radical site formed during the redox cycle¹. *J. Mol. Biol.* 286:809-827.
- Chung, N. and Aust, S.D. 1995. Veratryl alcohol-mediated indirect oxidation of phenol by lignin peroxidase. *Arch. Biochem. Biophys.* 316:733-737.

- Conesa, A., Punt, P.J., and Van Den Hondel, C.A. 2002. Fungal peroxidases: molecular aspects and applications. *J. Biotechnol.* 93:143-158.
- Cullen, D. and Kersten, P.J. 2004. Enzymology and molecular biology of lignin degradation. *Biochemistry and molecular biology*, 2nd Edition, ed. Esser, K.: Springer-Verlag New York LLC; Springer-Verlag GmbH & Co. KG. 249-273.
- Dean, R., Talbot, N., Ebbole, D., Farman, M., Mitchell, T., Orbach, M., Thon, M., Kulkarni, R., Xu, J., and Pan, H. 2005. The genome sequence of the rice blast fungus *Magnaporthe grisea*. *Nature* 434:980-986.
- DeLano, W.L. 2002. The PyMOL molecular graphics system. San Carlos, CA: DeLano Scientific.
- Dey, S., Maiti, T.K., and Bhattacharyya, B.C. 1994. Production of some extracellular enzymes by a lignin peroxidase-producing brown rot fungus, *Polyporus ostreiformis*, and its comparative abilities for lignin degradation and dye decolorization. *Appl. Environ. Microbiol.* 60:4216-4218.
- Dunford, H.B. and Stillman, J.S. 1976. On the function and mechanism of action of peroxidases. *Coordination Chemistry Reviews* 19:187-251.
- Eaton, R.A. and Hale, M.D.C. 1993. *Wood: decay, pests and protection*: Chapman and Hall Ltd.
- Enoki, A., Tanaka, H., and Fuse, G. 1988. Degradation of lignin-related compounds, pure cellulose, and wood components by white-rot and brown-rot fungi. *Holzforschung* 42:85-93.
- Eriksson, K.E.L., Blanchette, R.A., and Ander, P. 1990. *Microbial and enzymatic degradation of wood and wood components*: Springer-verlag.
- Faison, B. and Kirk, T. 1985. Factors involved in the regulation of a ligninase activity in *Phanerochaete chrysosporium*. *Appl. Environ. Microbiol.* 49:299-304.

- Fenn, P. and Kent Kirk, T. 1981. Relationship of nitrogen to the onset and suppression of ligninolytic activity and secondary metabolism in *Phanerochaete chrysosporium*. Arch. Microbiol. 130:59-65.
- Floudas, D., Binder, M., Riley, R., Barry, K., Blanchette, R.A., Henrissat, B., Martínez, A.T., Otilar, R., Spatafora, J.W., and Yadav, J.S. 2012. The Paleozoic origin of enzymatic lignin decomposition reconstructed from 31 fungal genomes. Science 336:1715-1719.
- Gettemy, J.M., Ma, B., Alic, M., and Gold, M.H. 1998. Reverse transcription-PCR analysis of the regulation of the manganese peroxidase gene family. Appl. Environ. Microbiol. 64:569.
- Giardina, P., Palmieri, G., Fontanella, B., Riviaccio, V., and Sannia, G. 2000. Manganese peroxidase isoenzymes produced by *Pleurotus ostreatus* grown on wood sawdust. Arch. Biochem. Biophys. 376:171-179.
- Gilbertson, R.L. 1980. Wood-rotting fungi of North America. Mycologia 72:1-49.
- Godfrey, B.J., Mayfield, M.B., Brown, J.A., and Gold, M.H. 1990. Characterization of a gene encoding a manganese peroxidase from *Phanerochaete chrysosporium*. Gene 93:119-124.
- Goodell, B. 2003. *Brown-rot fungal degradation of wood: our evolving view*. ACS Publications.
- Goodell, B., Jellison, J., Liu, J., Daniel, G., Paszczynski, A., Fekete, F., Krishnamurthy, S., Jun, L., and Xu, G. 1997. Low molecular weight chelators and phenolic compounds isolated from wood decay fungi and their role in the fungal biodegradation of wood. J. Biotechnol. 53:133-162.
- Goodell, B., Nicholas, D.D., Schultz, T.P., and Meeting, A.C.S. 2003. Wood deterioration and preservation: advances in our changing world: American Chemical Society.

- Hakala, T.K., Hildén, K., Maijala, P., Olsson, C., and Hatakka, A. 2006. Differential regulation of manganese peroxidases and characterization of two variable MnP encoding genes in the white-rot fungus *Physisporinus rivulosus*. *Appl. Microbiol. Biotechnol.* 73:839-849.
- Hall, B.G. 2007. *Phylogenetic trees made easy: a how-to manual*: Sinauer Associates, Inc.
- Hammel, K.E., Tardone, P.J., Moen, M.A., and Price, L.A. 1989. Biomimetic oxidation of nonphenolic lignin models by Mn (III): new observations on the oxidizability of guaiacyl and syringyl substructures. *Arch. Biochem. Biophys.* 270:404-409.
- Harvey, P.J., Palmer, J.M., Schoemaker, H.E., Dekker, H.L., and Wever, R. 1989. Pre-steady-state kinetic study on the formation of compound I and II of ligninase. *Biochim. Biophys. Acta, Protein Struct. Mol. Enzymol.* 994:59-63.
- Heinfling, A., Ruiz-Dueñas, F.J., Martínez, M.J., Bergbauer, M., Szewzyk, U., and Martínez, A.T. 1998. A study on reducing substrates of manganese-oxidizing peroxidases from *Pleurotus eryngii* and *Bjerkandera adusta*. *FEBS Lett.* 428:141-146.
- Hibbett, D.S. 2006. A phylogenetic overview of the Agaricomycotina. *Mycologia* 98:917-925.
- Hibbett, D.S. and Donoghue, M.J. 2001. Analysis of character correlations among wood decay mechanisms, mating systems, and substrate ranges in homobasidiomycetes. *Syst. Biol.* 50:215.
- Hildén, K., Martinez, A.T., Hatakka, A., and Lundell, T. 2005. The two manganese peroxidases Pr-MnP2 and Pr-MnP3 of *Phlebia radiata*, a lignin-degrading basidiomycete, are phylogenetically and structurally divergent. *Fungal Genet. Biol.* 42:403-419.

- Hilden, K.S., Makela, M.R., Hakala, T.K., Hatakka, A., and Lundell, T. 2006. Expression on wood, molecular cloning and characterization of three lignin peroxidase (LiP) encoding genes of the white rot fungus *Phlebia radiata*. *Curr. Genet.* 49:97-105.
- Hon, D.N.S. and Shiraishi, N. 2001. *Wood and cellulosic chemistry*. New York: Marcel Dekker.
- Houborg, K., Harris, P., Poulsen, J.C.N., Schneider, P., Svendsen, A., and Larsen, S. 2003. The structure of a mutant enzyme of *Coprinus cinereus* peroxidase provides an understanding of its increased thermostability. *Acta Crystallogr. Sect. D. Biol. Crystallogr.* 59:997-1003.
- Huang, S., Tzean, S., Tsai, B., and Hsieh, H. 2009. Cloning and heterologous expression of a novel ligninolytic peroxidase gene from poroid brown-rot fungus *Antrodia cinnamomea*. *Microbiology* 155:424.
- Huang, S.T. 2008. Cloning and heterologous expression of a novel ligninolytic peroxidase gene from poroid brown-rot fungus *Antrodia cinnamomea* and a versatile peroxidase gene from poroid white-rot fungus *Ganoderma lucidum*, in Department of Plant Pathology and Microbiology College of Bioresources and Agriculture. National Taiwan University.
- Huelsenbeck, J.P. and Ronquist, F. 2001. MRBAYES: Bayesian inference of phylogenetic trees. *Bioinformatics* 17:754-755.
- Irie, T., Honda, Y., Ha, H.C., Watanabe, T., and Kuwahara, M. 2000. Isolation of cDNA and genomic fragments encoding the major manganese peroxidase isozyme from the white rot basidiomycete *Pleurotus ostreatus*. *J. Wood Sci.* 46:230-233.
- Jönsson, L. and Nyman, P.O. 1994. Tandem lignin peroxidase genes of the fungus *Trametes versicolor*. *Biochimica et Biophysica Acta (BBA)-Gene Structure and Expression* 1218:408-412.

- James, T.Y., Srivilai, P., Kües, U., and Vilgalys, R. 2006. Evolution of the bipolar mating system of the mushroom *Coprinellus disseminatus* from its tetrapolar ancestors involves loss of mating-type-specific pheromone receptor function. *Genetics* 172:1877-1891.
- Jeffries, T.W., Choi, S., and Kirk, T.K. 1981. Nutritional regulation of lignin degradation by *Phanerochaete chrysosporium*. *Appl. Environ. Microbiol.* 42:290-296.
- Johansson, T. and Nyman, P.O. 1995. The gene from the white-rot fungus *Trametes versicolor* encoding the lignin peroxidase isozyme LP7. *Biochimica et Biophysica Acta (BBA)-Gene Structure and Expression* 1263:71-74.
- Johansson, T., Nyman, P.O., and Cullen, D. 2002. Differential regulation of *mnp2*, a new manganese peroxidase-encoding gene from the ligninolytic fungus *Trametes versicolor* PRL 572. *Appl. Environ. Microbiol.* 68:2077-2080.
- Jonsson, L. and Nyman, P. 1992. Characterization of a lignin peroxidase gene from the white-rot fungus *Trametes versicolor*. *Biochimie* 74:177-182.
- Keyser, P., Kirk, T., and Zeikus, J. 1978. Ligninolytic enzyme system of *Phanaerochaete chrysosporium*: synthesized in the absence of lignin in response to nitrogen starvation. *J. Bacteriol.* 135:790-797.
- Kim, Y., Yeo, S., Kum, J., Song, H., and Choi, H.T. 2005. Cloning of a manganese peroxidase cDNA gene repressed by manganese in *Trametes versicolor*. *J. Micorbio.* 43:569.
- Kimura, Y., Asada, Y., Oka, T., and Kuwahara, M. 1991. Molecular analysis of a *Bjerkandera adusta* lignin peroxidase gene. *Appl. Microbiol. Biotechnol.* 35:510-514.

- Kirk, T.K., Schultz, E., Connors, W., Lorenz, L., and Zeikus, J. 1978. Influence of culture parameters on lignin metabolism by *Phanerochaete chrysosporium*. Arch. Microbiol. 117:277-285.
- Kishi, K., Kusters-van Someren, M., Mayfield, M.B., Sun, J., Loehr, T.M., and Gold, M.H. 1996. Characterization of manganese (II) binding site mutants of manganese peroxidase. Biochemistry (Mosc). 35:8986-8994.
- Kjalke, M., Andersen, M.B., Schneider, P., Christensen, B., Schulein, M., and Welinder, K.G. 1992. Comparison of structure and activities of peroxidases from *Coprinus cinereus*, *Coprinus macrorhizus* and *Arthromyces ramosus*. Biochim. Biophys. Acta, Protein Struct. Mol. Enzymol. 1120:248-256.
- Koduri, R.S. and Tien, M. 1994. Kinetic analysis of lignin peroxidase: explanation for the mediation phenomenon by veratryl alcohol. Biochemistry (Mosc). 33:4225-4230.
- Kuila, D., Tien, M., Fee, J.A., and Ondrias, M.R. 1985. Resonance Raman spectra of extracellular ligninase: evidence for a heme active site similar to those of peroxidases. Biochemistry (Mosc). 24:3394-3397.
- Kuwahara, M., Glenn, J.K., Morgan, M.A., and Gold, M.H. 1984. Separation and characterization of two extracellular H₂O₂-dependent oxidases from ligninolytic cultures of *Phanerochaete chrysosporium*. FEBS Lett. 169:247-250.
- Lankinen, P., Hilden, K., Aro, N., Salkinoja-Salonen, M., and Hatakka, A. 2005. Manganese peroxidase of *Agaricus bisporus*: grain bran-promoted production and gene characterization. Appl. Microbiol. Biotechnol. 66:401-407.
- Larkin, M., Blackshields, G., Brown, N., Chenna, R., McGettigan, P., McWilliam, H., Valentin, F., Wallace, I., Wilm, A., and Lopez, R. 2007. Clustal W and Clustal X version 2.0. Bioinformatics 23:2947-2948.

- Levasseur, A., Piumi, F., Coutinho, P., Rancurel, C., Asther, M., Delattre, M., Henrissat, B., Pontarotti, P., and Record, E. 2008. FOLy: an integrated database for the classification and functional annotation of fungal oxidoreductases potentially involved in the degradation of lignin and related aromatic compounds. *Fungal Genet. Biol.* 45:638-645.
- Li, D., Alic, M., and Gold, M.H. 1994. Nitrogen regulation of lignin peroxidase gene transcription. *Appl. Environ. Microbiol.* 60:3447-3449.
- Li, D., Li, N., Ma, B., Mayfield, M.B., and Gold, M.H. 1999. Characterization of genes encoding two manganese peroxidases from the lignin-degrading fungus *Dichomitus squalens*1. *Biochim. Biophys. Acta, Protein Struct. Mol. Enzymol.* 1434:356-364.
- Lobos, S., Larrondo, L., Salas, L., Karahanian, E., and Vicuña, R. 1998. Cloning and molecular analysis of a cDNA and the Cs-mnp1 gene encoding a manganese peroxidase isoenzyme from the lignin-degrading basidiomycete *Ceriporiopsis subvermispora*. *Gene* 206:185-193.
- Ma, B., Mayfield, M.B., Godfrey, B.J., and Gold, M.H. 2004. Novel promoter sequence required for manganese regulation of manganese peroxidase isozyme 1 gene expression in *Phanerochaete chrysosporium*. *Eukaryot. Cell* 3:579-588.
- Martin, F., Aerts, A., Ahren, D., Brun, A., Danchin, E., Duchaussoy, F., Gibon, J., Kohler, A., Lindquist, E., and Pereda, V. 2008. The genome of *Laccaria bicolor* provides insights into mycorrhizal symbiosis. *Nature* 452:88-92.
- Martinez, D., Challacombe, J., Morgenstern, I., Hibbett, D., Schmoll, M., Kubicek, C.P., Ferreira, P., Ruiz-Duenas, F.J., Martinez, A.T., and Kersten, P. 2009. Genome, transcriptome, and secretome analysis of wood decay fungus *Postia placenta* supports unique mechanisms of lignocellulose conversion. *Proc. Natl. Acad. Sci.* 106:1954.

- Martinez, D., Larrondo, L.F., Putnam, N., Gelpke, M.D.S., Huang, K., Chapman, J., Helfenbein, K.G., Ramaiya, P., Detter, J.C., and Larimer, F. 2004. Genome sequence of the lignocellulose degrading fungus *Phanerochaete chrysosporium* strain RP78. *Nat. Biotechnol.* 22:695-700.
- Martinez, M.J., Ruiz-Dueñas, F.J., Guillén, F., and Martinez, A.T. 1996. Purification and catalytic properties of two manganese peroxidase isoenzymes from *Pleurotus eryngii*. *Eur. J. Biochem.* 237:424-432.
- Mayfield, M.B., Godfrey, B.J., and Gold, M.H. 1994. Characterization of the *mnp2* gene encoding manganese peroxidase isozyme 2 from the basidiomycete *Phanerochaete chrysosporium*. *Gene* 142:231-235.
- Mester, T., De Jong, E., and Field, J.A. 1995. Manganese regulation of veratryl alcohol in white rot fungi and its indirect effect on lignin peroxidase. *Appl. Environ. Microbiol.* 61:1881.
- Mester, T. and Field, J.A. 1998. Characterization of a novel manganese peroxidase-lignin peroxidase hybrid isozyme produced by *Bjerkandera* species strain BOS55 in the absence of manganese. *J. Biol. Chem.* 273:15412-15417.
- Moreira, P.R., Duez, C., Dehareng, D., Antunes, A., Almeida-Vara, E., Frère, J.M., Malcata, F.X., and Duarte, J. 2005. Molecular characterisation of a versatile peroxidase from a *Bjerkandera* strain. *J. Biotechnol.* 118:339-352.
- Morgenstern, I., Klopman, S., and Hibbett, D.S. 2008. Molecular evolution and diversity of lignin degrading heme peroxidases in the Agaricomycetes. *J. Mol. Evol.* 66:243-257.
- Morgenstern, I., Robertson, D.L., and Hibbett, D.S. 2010. Characterization of Three *mnp* Genes of *Fomitiporia mediterranea* and Report of Additional Class II Peroxidases in the Order Hymenochaetales. *Appl. Environ. Microbiol.* 76:6431-6440.

- Nagai, M., Sakamoto, Y., Nakade, K., and Sato, T. 2007. Isolation and characterization of the gene encoding a manganese peroxidase from *Lentinula edodes*. *Mycoscience* 48:125-130.
- Naidu, P.S., Zhang, Y.Z., and Reddy, C.A. 1990. Characterization of a new lignin peroxidase gene (GLG6) from *Phanerochaete chrysosporium*. *Biochem. Biophys. Res. Commun.* 173:994-1000.
- Niemenmaa, O., Uusi-Rauva, A., and Hatakka, A. 2008. Demethoxylation of [$O_{14}CH_3$]-labelled lignin model compounds by the brown-rot fungi *Gloeophyllum trabeum* and *Poria (Postia) placenta*. *Biodegradation* 19:555-565.
- Paterson, A., McCarthy, A., and Broda, P. 1984. The application of molecular biology to lignin degradation. *Soc. Appl. Bacteriol. Tech. Ser.* 19:33-68.
- Pease, E.A. and Tien, M. 1992. Heterogeneity and regulation of manganese peroxidases from *Phanerochaete chrysosporium*. *J. Bacteriol.* 174:3532-3540.
- Pointing, S.B., Pelling, A.L., Smith, G.J.D., Hyde, K.D., and Reddy, C.A. 2005. Screening of basidiomycetes and xylariaceous fungi for lignin peroxidase and laccase gene-specific sequences. *Mycol. Res.* 109:115-124.
- Poulos, T., Edwards, S., Wariishi, H., and Gold, M. 1993. Crystallographic refinement of lignin peroxidase at 2 Å. *J. Biol. Chem.* 268:4429-4440.
- Poulos, T.L. and Kraut, J. 1980. The stereochemistry of peroxidase catalysis. *J. Biol. Chem.* 255:8199-8205.
- Pribnow, D., Mayfield, M.B., Nipper, V.J., Brown, J.A., and Gold, M.H. 1989. Characterization of a cDNA encoding a manganese peroxidase, from the lignin-degrading basidiomycete *Phanerochaete chrysosporium*. *J. Biol. Chem.* 264:5036.
- Rubin, E.M. 2008. Genomics of cellulosic biofuels. *Nature* 454:841-845.

- Ruiz-Duenas, F., Camarero, S., Perez-Boada, M., Martinez, M., and Martinez, A. 2001. A new versatile peroxidase from *Pleurotus*. *Biochem. Soc. Trans.* 29:116.
- Ruiz-Dueñas, F.J., Martínez, M.J., and Martínez, A.T. 1999. Molecular characterization of a novel peroxidase isolated from the ligninolytic fungus *Pleurotus eryngii*. *Mol. Microbiol.* 31:223-235.
- Sachs, I.B., Clark, I.T., and Pew, J.C. Investigation of lignin distribution in the cell wall of certain woods. 1963: Wiley Online Library.
- Sakakibara, A. 1980. A structural model of softwood lignin. *Wood Science and Technology* 14:89-100.
- Sakamoto, Y., Nakade, K., Nagai, M., Uchimiya, H., and Sato, T. 2009. Cloning of *Lentinula edodes* lemnp2, a manganese peroxidase that is secreted abundantly in sawdust medium. *Mycoscience* 50:116-122.
- Saloheimo, M., Barajas, V., Niku-Paavola, M.L., and Knowles, J.K.C. 1989. A lignin peroxidase-encoding cDNA from the white-rot fungus *Phlebia radiata*: characterization and expression in *Trichoderma reesei*. *Gene* 85:343-351.
- Sawai-Hatanaka, H., Ashikari, T., Tanaka, Y., Asada, Y., Nakayama, T., Minakata, H., Kunishima, N., Fukuyama, K., Yamada, H., and Shibano, Y. 1995. Cloning, sequencing, and heterologous expression of a gene coding for *Arthromyces ramosus* peroxidase. *Biosci., Biotechnol., Biochem.* 59:1221-1228.
- Schwarze, F.W.M.R., Engels, J., and Mattheck, C. 2000. Fungal strategies of wood decay in trees: Springer Verlag.
- Sjöström, E. 1993. Wood chemistry: fundamentals and applications. New York: Academic Press.
- Stajich, J.E., Wilke, S.K., Ahrén, D., Au, C.H., Birren, B.W., Borodovsky, M., Burns, C., Canbäck, B., Casselton, L.A., and Cheng, C. 2010. Insights into evolution of

- multicellular fungi from the assembled chromosomes of the mushroom *Coprinopsis cinerea* (*Coprinus cinereus*). Proc. Natl. Acad. Sci. 107:11889.
- Stamatakis, A., Hoover, P., and Rougemont, J. 2008. A rapid bootstrap algorithm for the RAxML Web servers. Syst. Biol. 57:758-771.
- Sue Yaver, D., Weber, B., and Murrell, J. 2003. Global expression profiling of the lignin degrading fungus *Ceriporiopsis subvermispora* for the discovery of novel enzymes. Applied Mycology and Biotechnology 3:261-269.
- Sugiura, T., Yamagishi, K., Kimura, T., Nishida, T., Kawagishi, H., and Hirai, H. 2009. Cloning and homologous expression of novel lignin peroxidase genes in the white-rot fungus *Phanerochaete sordida* YK-624. Biosci., Biotechnol., Biochem. 73:1793-1798.
- Sundaramoorthy, M., Kishi, K., Gold, M.H., and Poulos, T.L. 1994. The crystal structure of manganese peroxidase from *Phanerochaete chrysosporium* at 2.06-Å resolution. J. Biol. Chem. 269:32759-32767.
- Sutherland, G.R.J. and Aust, S.D. 1996. The effects of calcium on the thermal stability and activity of manganese peroxidase. Arch. Biochem. Biophys. 332:128-134.
- Szklarz, G.D., Antibus, R.K., Sinsabaugh, R.L., and Linkins, A.E. 1989. Production of phenol oxidases and peroxidases by wood-rotting fungi. Mycologia:234-240.
- Tamura, K., Peterson, D., Peterson, N., Stecher, G., Nei, M., and Kumar, S. 2011. MEGA5: molecular evolutionary genetics analysis using maximum likelihood, evolutionary distance, and maximum parsimony methods. Mol. Biol. Evol. 28:2731-2739.
- Tello, M., Corsini, G., Larrondo, L.F., Salas, L., Lobos, S., and Viciña, R. 2000. Characterization of three new manganese peroxidase genes from the ligninolytic basidiomycete *Ceriporiopsis subvermispora*. Biochimica et Biophysica Acta (BBA)-Gene Structure and Expression 1490:137-144.

- Terashima, N., Atalla, R.H., and Vanderhart, D.L. 1997. Solid state NMR spectroscopy of specifically ^{13}C -enriched lignin in wheat straw from coniferin. *Phytochemistry* 46:863-870.
- Terauchi, R. and Kahl, G. 2000. Rapid isolation of promoter sequences by TAIL-PCR: the 5'-flanking regions of Pal and Pgi genes from yams (*Dioscorea*). *Mol. Gen. Genet.* 263:554-560.
- Tien, M., Kirk, T.K., Bull, C., and Fee, J.A. 1986. Steady-state and transient-state kinetic studies on the oxidation of 3, 4-dimethoxybenzyl alcohol catalyzed by the ligninase of *Phanerochaete chrysosporium* Burds. *J. Biol. Chem.* 261:1687-1693.
- Tien, M. and Tu, C.P.D. 1987. Cloning and sequencing of a cDNA for a ligninase from *Phanerochaete chrysosporium*. *Nature* 326:520-523.
- Tonon, F. and Odier, E. 1988. Influence of veratryl alcohol and hydrogen peroxide on ligninase activity and ligninase production by *Phanerochaete chrysosporium*. *Appl. Environ. Microbiol.* 54:466-472.
- Valli, K., Wariishi, H., and Gold, M.H. 1990. Oxidation of monomethoxylated aromatic compounds by lignin peroxidase: role of veratryl alcohol in lignin biodegradation. *Biochemistry (Mosc).* 29:8535-8539.
- Wariishi, H., Akileswaran, L., and Gold, M.H. 1988. Manganese peroxidase from the basidiomycete *Phanerochaete chrysosporium*: spectral characterization of the oxidized states and the catalytic cycle. *Biochemistry (Mosc).* 27:5365-5370.
- Welinder, K.G. 1992. Superfamily of plant, fungal and bacterial peroxidases. *Curr. Opin. Struct. Biol.* 2:388-393.
- Whitwam, R.E., Brown, K.R., Musick, M., Natan, M.J., and Tien, M. 1997. Mutagenesis of the Mn^{2+} -binding site of manganese peroxidase affects oxidation of Mn^{2+} by both compound I and compound II. *Biochemistry (Mosc).* 36:9766-9773.

Worrall, J.J., Anagnost, S.E., and Zabel, R.A. 1997. Comparison of wood decay among diverse lignicolous fungi. *Mycologia*:199-219.



Table 1. Fungal species used in basal peroxidase gene cloning and characterization.

Family	Species	Strain	Other Collection No.	Source	Rot type ^a
Gloeophyllales	<i>Gloeophyllum trabeum</i>	BCRC31614	(= ATCC 32084 ;DSM 1398)	Canada	B
Polyporales	<i>Laetiporus sulphureus</i>	BCRC36870	(= CBS 608.74)	Netherlands	B
Polyporales	<i>Antrodia salmonea</i>	TFRI B147		Hsinchu County, Taiwan	B
Polyporales	<i>Antrodia xantha</i>				B
Polyporales	<i>Fomitopsis pinicola</i>	BCRC35664		Taichung, Taiwan	B
Polyporales	<i>Ganoderma australe</i>	BCRC35394	(= TFRI 17)	Pingtung, Taiwan	W
Hymenochaetales	<i>Phellinus noxius</i>	BCRC35248	(= ATCC 200093)	Kaohsiung, Taiwan	W
Polyporales	<i>Trametes versicolor</i>				W
Polyporales	<i>Phanerochaete chrysosporium</i>	BCRC36200	(= ATCC 24725 ; = CBS 481.73 ; = CMI 174727 ; = NRRL 6361)		W
Agaricales	<i>Agaricus bisporus</i>	BCRC36219			W
Polyporales	<i>Pycnoporus sanguineus</i>	BCRC35298		Nantou, Taiwan	W
Ophiostomatales	<i>Ophiostoma quercus</i> ^b	OPH110		Taichung, Taiwan	-

a. B: brown rot fungi; W: white rot fungi

b. Ascomycetes

Table 2. Primers used in this study

Name	Sequence (5' → 3')	Application
lips_1 ^a	CATGAAGTCAGCTAYGGNGAY	<i>BaP</i> cloning
lips_2 ^a	GAATGGCAGAYGCNNGNTTY	<i>BaP</i> cloning
lipr_3 ^a	GTCGTGCCCTTGRTTNGCNARYTT	<i>BaP</i> cloning
lipr_4 ^a	GGGTATGACRAANSWRCARTC	<i>BaP</i> cloning
Aslnp_RS	AGACGCTGGGTTC AACGCGGGAGATAC	RACE ^b
Aslnp_RR	GAGTGTCGAATATTTTGGGGGTGCTGTC	RACE ^c
		Southern blot probe
ITS4	TCCTCCGCTTATTGATATGC	Identification
ITS5	GGAAGTAAAAGTCGTAACAAGG	Identification
Lslnp_RS	CTCATGGCAGCGCACTCGGTCGCCGTAC	RACE ^d
Lslnp_RR	CGCTCTTGATCGACGAACGCTTCCCAGTA	RACE ^e
Lslnp_FS	GGCACATACATCCAGAGCGGATCAA	<i>LsBaP</i> cloning
Lslnp_FR	CCCGCCATCAAATCTAAGCATCGCA	<i>LsBaP</i> cloning
Ls_t5_A	GGCACTTGCCTGCACCTCCTCC	Tail-PCR
Ls_t5_B	TTCCTGGCTGGATCGCCGCATTTT	Tail-PCR
Ls_t5_C1	TCCCGCCATCAAATCTAAGCATCG	Tail-PCR
Ls_t5_C2	TGTTTTTCGTCACAAGAAGCCAGC	Tail-PCR
Ls_t5_C3	ACCAGCGGTTGCACTGAGAGATTG	Tail-PCR
G0427F	TGCTGGAGCTGTGGCCCTCTCGAACTGTC	Southern blot probe
qGA_F	CCACGACCGAGACATCAAT	qPCR
qGA_R	CAGTCGGCAACAACATCATC	qPCR
1018F	GGTTCACAGCGGAGGACAC	qPCR
1018R	ACTGCGAGTCAAAGGCTTCC	qPCR

a. degenerate primer

b. gene specific primer for *A. salmonella* 5' RACE

c. gene specific primer for *A. salmonella* 3' RACE

d. gene specific primer for *L. sulphureus* 5' RACE

e. gene specific primer for *L. sulphureus* 3' RACE

Table 3. Reaction parameters for the tail-PCR

PCR Round	Primers	Cycle parameters
1 st round	Ls_t5_A	93°C, 1 min; 95°C, 1 min for 1 cycle 94°C, 30 s; 62°C, 1 min; 72°C, 2.5 min for 5 cycle 94°C, 30 s; 25°C, 3 min; 72°C 3 min; 72°C, 2.5 min; 94°C, 10 s; 29°C, 1min; 72°C, 2.5 min for 15cycle 72°C, 5 min for 1 cycle
2 nd round	Ls_t5_B	94°C, 10 s; 64°C, 1 min; 72°C, 2.5 min; 94°C, 10 s; 64°C, 1 min; 72°C, 2.5 min; 94°C, 10 s; 29°C, 1 min; 72°C, 2.5 min for 12 cycles 72°C, 5 min for 1 cycles
3 rd round	Ls_t5_C1 Ls_t5_C2 Ls_t5_C3	94°C, 15 s; 29°C, 30 s; 72°C, 2 min for 20 cycles 72°C, 5 min for 1 cycle



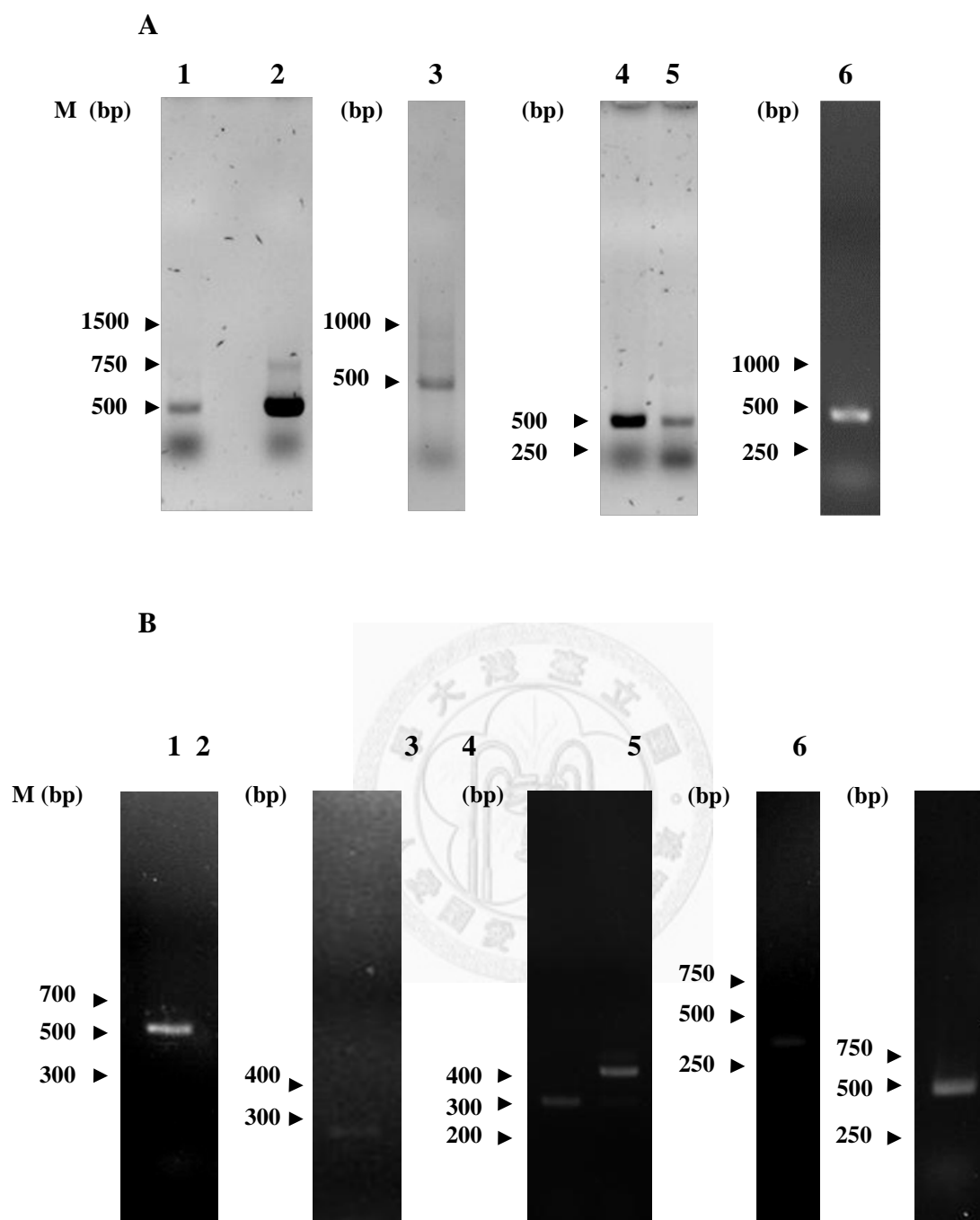


Fig. 1. Putative basal peroxidase gene cloned from brown rot and white rot fungi by degenerate primers.

(A) Brown rot fungi. Lane 1: *Gloeophyllum trabeum*; Lane 2: *Antrodia salmonea*; Lane 3: *A. xantha*; Lane 4: *A. oleracea*; Lane 5: *Laetiporus sulphureus*; Lane 6: *Fomitopsis pinicola*. (B) White rot fungi. Lane 1: *Trametes versicolor*; Lane 2: *Phellinu snoxius*; Lane 3: *Pycnoporus sanguineus*; Lane 4: *Ganoderma australe*; Lane 5: *Phanerochaete chrysosporium*; Lane 6: *Agaricus bisporus*.

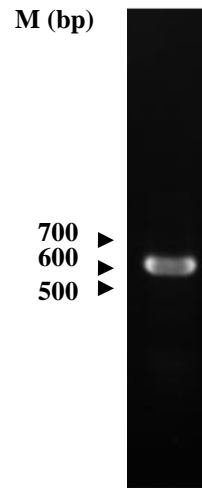
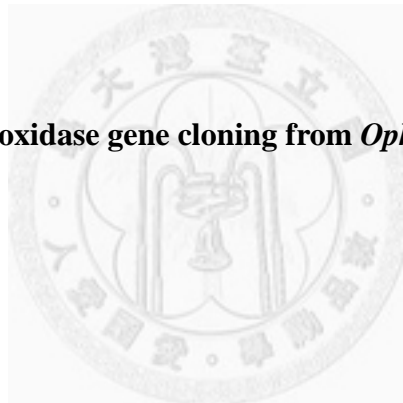


Fig. 2. Putative basal peroxidase gene cloning from *Ophiostoma quercus* by degenerate primers.



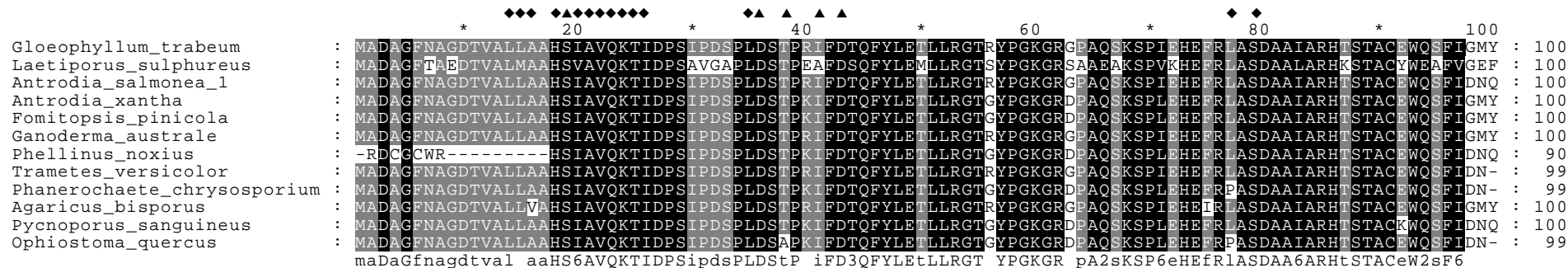


Figure 3. Traits of cloned basal peroxidase gene in target fungal species.

The characteristic domains were identified by blastx with conserved domain database (CDD), including heme binding site and calcium binding site within the deduced amino acid sequences. □ heme binding site; ▲ calcium binding site.

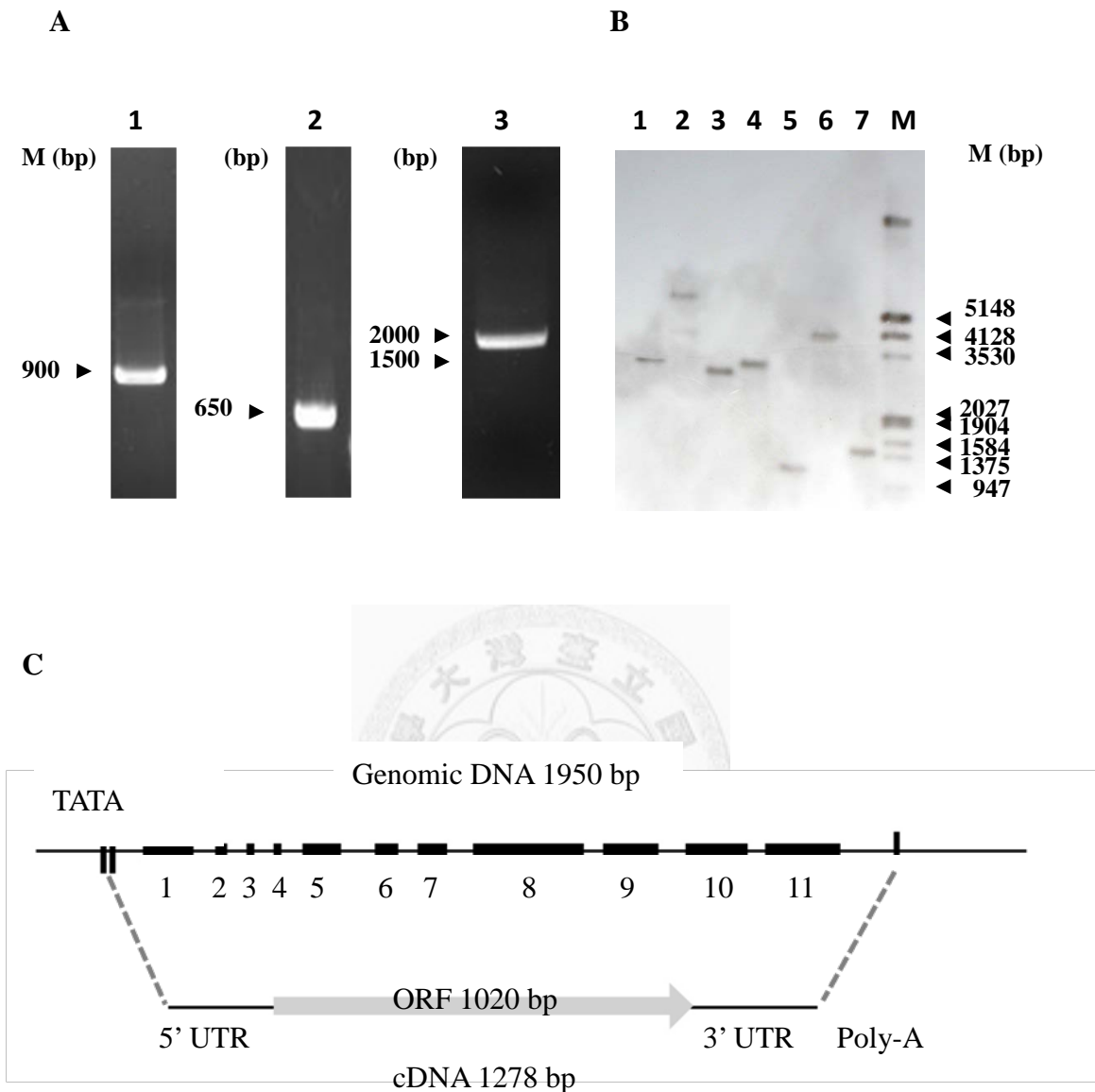


Fig. 4. The gene structure of *Laetiporus sulphureus* (Ls) *LsBaP*.

(A) Lane 1 and Lane 2 are 5' and 3' RACE amplicons amplified using *Lslnp_RS* and *Lslnp_RR* as primers respectively. The amplicon was analyzed by 1.5 % agarose gel. Lane3: *LsBaP* cDNA full length amplified by gene specific primers *Lslnp_FS* and *Lslnp_FR*. (B) Southern blot analysis of genomic DNA of *LsBaP*. Lane 1: digested by *AflIII*; Lane 2: digested by *PstI*; Lane 3: digested by *EcoRV*; Lane 4: digested by *HindIII*; Lane 5: digested by *PstI* and *AflIII*; Lane 6: digested by *EcoRV* and *HindIII*; Lane 7: digested by *AflIII* and *EcoRV*; Lane 8: digested by *PstI* and *EcoRV*. The hybridization was performed using probe generated by *Aslnp_RR* and G0427F primers.

-698 ggcacatacatccagagcggatcaaccagtcgtacgac

-660 ggggggaacacaccatgctgaagatcacaggcatcatgttcagcctcgacatggattgtggtggtacacatga
CSRE

-586 gtaacccatgtcgggtccaggggtatcagggcggcccgtgtcgaccgtgcgcgtgaagatgttctccgggacg
MRE

-514 aagacaccettattccacagcaaaatctgttcttgcgggcattcgtgttcgcagcgtgctgctcgcggacg
CSRE

-439 cgctgaaaccggtcgtagtaggcatcgggacgatggggtcgtcaagcatttgtgatgagaaggtctgctg

-366 catcgttgcgagcttctggcaaactagctcgtcatggaaaggtgggggggtatgaacttggagtaataacga

-292 ccaggcatggcgacggtggtgaggtgaggtcagggagagaaaatgggctcagcgtggagtcgcgctgcaa
MRE

-222 aagcacgctaatagacgatcagccagaagggtcgtctaaccggagttgggcgtctagaccgtaaacgtaaaa
TFIIB TATA box MTE

-150 atcgcgcgcgagacgcgaaaaagcctcccctaaactatagccatcacgtccaatacgcgtctcgctcgcac
▼

-77 gcgcctgcggctggaagcgtctcgcgtgttctgttattccatctagcttagattctgataatacatcacactctt
1 M F Y A Y W A A L L F L T H L

+1 ATGTTTTACGCGTATTGGGCTGCTCTACTTTTCCTGACGCATTGT

16 Y D C C V A S intron I

47 ATGATTGCTGTGTAGCCTCAAgtgcggcgcatttcgcttctgctgttcccgttacgctgact
23 T V H T E H S A A P S

112 cgcttgctaccaGCTGTACACACTGAGCATTCTGCAGCGCCATCAgtgagtagc
34 intron II C N R W F E

167 attattcaggatatatttcttgaagccagattcaatctctcagTGCAACCGCTGGTTCGAAgt
40 intron III I L D D L

234 gcgtgtgttctgctggcttctgtgacgaaaaacaatgaatcgctgcctagATTCTGGACGATCTT
45 Q S N V intron IV F

301 CAATCCAACGTgtaaacttatcaaactcgaacggtttggcatatgttgaatgcatgcttagATTT
50 D G G K C G D P A R K A L R L

369 GATGGCGGGAAATGCGGCGATCCAGCCAGGAAGGCACTTCGACTC

65 T F H D G I G R S A A L K A S G
 414 ACGTTTCATGACGGAATAGGTCGTTCTGCTGCTTTGAAAGCTTCTGG
 intron V
 461 Gagattccgtgcgtattcaaatacttaggcacactatcgtatggctcaacaacaagtagtggaggaggtgca
 81 R F P G G G
 534 ggcaagtgccattgtctggcagtacgcacggaaagctcacatatgAGATTTCCTGGAGGAGG
 87 A D G S I I K F A D V E L E D
 597 TGCAGACGGCAGCATCATCAAGTTTGCAGATGTCGAGCTAGAAGAC
 102 intron VI P A N I G
 643 cgtatgtacgtgcatcgtcgatatacccgactcatcggaaatcgtagCCGGCAAACATAGGCC
 107 L E G I V Y V L R S L A D G H G
 708 TGGAAGGCATAGTGTATGTTCTCAGATCTCTGGCCGATGGTCACGGT
 123 V S Y G D I intron VII
 755 GTGAGCTACGGCGACATgtgcgtattgtcgcttaatcgcggtcgcttaatccatgcgacctcage
 129 I Q F A G A V A L S
 820 gcatatactgaccagtggatgaagCATAACAATTTGCCGGAGCCGTGGCTCTGTCC
 137 N C P G S P R L A F Y A G R A
 875 AACTGTCCCGGAAGCCCTCGCCTCGCCTTCTACGCTGGACGTGCCG
 154 E A I A P A P P K L A P L P T
 921 AGGCGGATTGCCCCCGCTCCACCTAAGCTGGCCCCATTACCGACGG
 169 D S A E T I L S R M A D A G F T
 967 ATTCGGCGGAAACGATATTGTCTCGGATGGCAGATGCAGGGTTCAC
 185 P E D T V A L M A A H S V A V
 1013 ACCAGAGGACACGGTCGCGCTCATGGCAGCGCACTCGGTCGCCGT
 200 Q K T I D P S A V G A P L D S
 1058 ACAAAGACTATCGATCCTAGCGCAGTTGGCGCACCGTTGGACAGC
 215 T P E V F D S Q F Y L E
 1104 ACGCCGGAAGTCTTTGACTCGCAGTTCTACTTGGAggtatgttgagagcgaca
 227 intron VIII M L L R G T S Y
 1157 tgcgaagetccgctaacctaatctccttgacgaGATGCTCCTTAGGGGCACCAGCTACC
 235 P G K G R S A A E A K S P V K
 1216 CCGGTAAAGGGAGATCAGCGGCGGAGGCGAAGTCACCTGTGAAGC
 250 H E F R L A S D A A L A R H K S

ACGAATTCCGACTGGCATCGGATGCCGCGCTTGCACGGCATAAAAG
266 T A C Y W E A F V
 1307 CACCGCTTGCTACTGGGAAGCGTTCGTCggtgagttccgaatatcccgtgtacaagat
275 intron IX G D Q E R
 1365 caactggtgggaatacctcgtgtcctgacgtgactgccgcgctacaGGTGATCAAGAGCGTA
280 M R G S F R K A M E K L A N Q
 1429 TGC GCGGATCCTTCCGAAAAGCCATGGAGAAGCTCGCGAATCAGG
295 G H S N L A D C S S V I P V P K
 1474 GCCATTCAAATCTCGCCGATTGTTTCGTCTGTCATTCCCGTTCCGAAA
311 P W S R P P T L P R G K N I S
 1521 CCTTGGAGCCGCCCGCCTACGTTGCCTCGAGGCAAGAACATCTCGG
326 D I E Q T intron X
 1567 ATATCGAACAGACTgtgagtcgtttgcgcctcgcaggcacccctgacacctccgccctatgctgat
331 C T A V Q F P P L A*
 1633 ggacgccgtagTGTACGGCAGTCCAATTCCCCCCTCTAGCCTAAccctgcaca
 1687 tcgtacacagctgtcccggccctatgtcggaggacttctcatgcagcttttctcattattgctatgtcccagct
 1763 gaatgccaatcctagcattaatgtgattgtgtcgcgtgtctgaaatgccaatttgaggattcaggaggagc
 1836 agtgtga

Fig. 5. Nucleotide and translated amino acid sequences of basal peroxidase gene of *L. sulphureus* (*LsBaP*).

Exons indicated by upper case letter and introns I-X in lower case letter letters. Beginning of the transcript is shown in ▼ and the stop codon is marked with *. 5' promoter sequence is numbered negatively from transcriptional starting site. Amino acids are numbered in boldface. 3' UTR is marked in italics. The putative signal peptide is marked with shading block. The asterisk indicate heme binding site including proximal and distal histidine. Putative transcription factor binding sites are underlined. MTE: Core promoter motif ten elements; TFIIB: RNA polymerase II transcription factor II B; MRE: Metal regulatory element factor; CSRE: Carbon source-responsive elements.

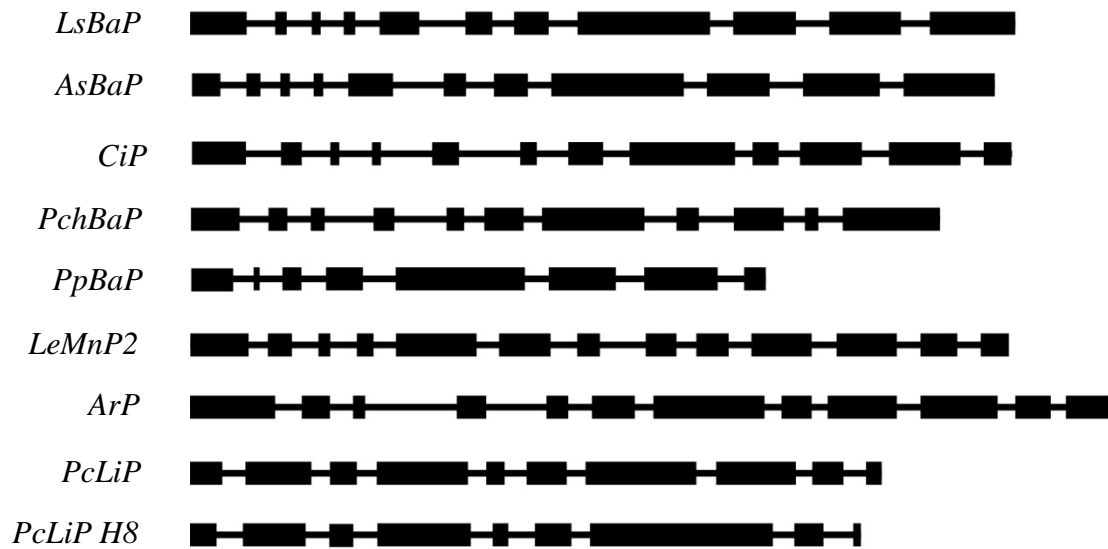


Fig. 6. The exon / introns distribution of basal peroxidase, lignin peroxidase, manganese peroxidase, CiP and ARP in nine white and brown rot Basidiomycetes:

Figure were drawn in proportion to gene length. Black boxes and line fragments represent exon and introns respectively. The exon / introns distribution are conserved between *LsBaP* and *AsBaP*. In contract to lignin peroxidase gene *PcLiP* and *PcLiP H8*, several small exon in size about 25-50 bp in size located within near 5' terminal region of *LsBaP*, *AsBaP*, *CiP*, *PchBaP*, *PpBaP* and *LeMnP2*. Abbreviations: *Laetiporus sulphureus* (*LsBaP*), *Antrodia salmonea* (*AsBaP*), *Coprinus cinerea* (*CiP*), *Phanerochaete chrysosporium* (*PchBaP*, *PcLiP*, *PcLiP H8*), *Postia placenta* (*PpBaP*), *Lentinus edodes* (*LeMnP2*), *Arthromyces ramosus* (*ArP*).

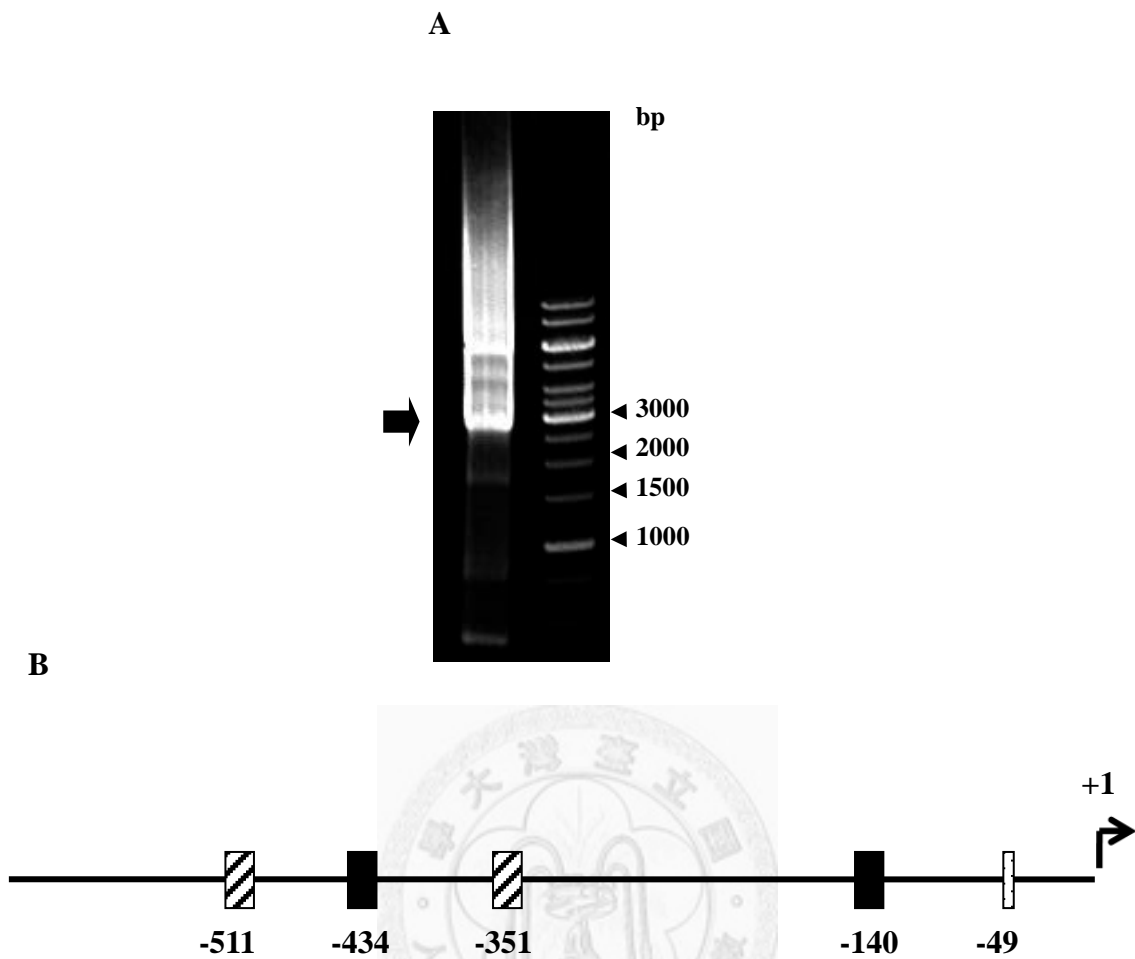


Fig. 7. The analysis of *LsBaP* promoter.

(A) 5' unknown region amplified by tail-PCR. The bold arrow indicate predicted product (~ 3.0kb); arrow heads indicate nucleotide base pairs. (B) Two important transcription factor binding sites. ■ : metal regulatory element factors (MREs); ▨ : carbon source-responsive elements; □ : TATA box.

RQ

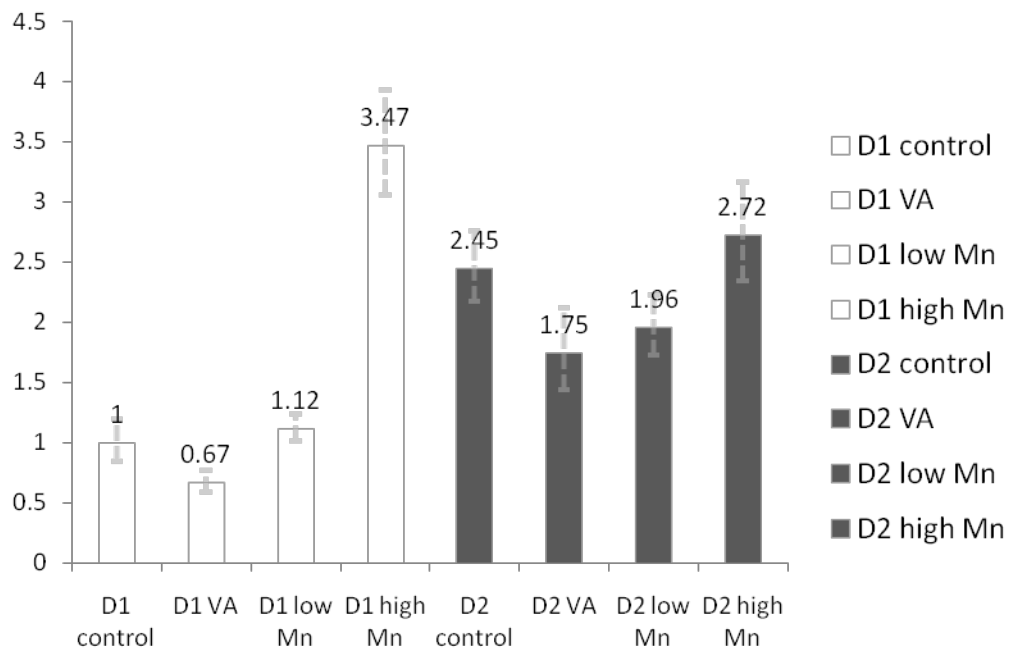


Fig. 8. The quantitative RT-PCR analysis of *LsBaP*.

The prevalence of transcript of *LsBaP* under different culture conditions: Mn-free (control), Mn-free with VA, 18 μM Mn and 180 μM Mn medium at day1 (D1) and day 2 (D2). The qRT-PCR was performed using GAPDH as internal control.

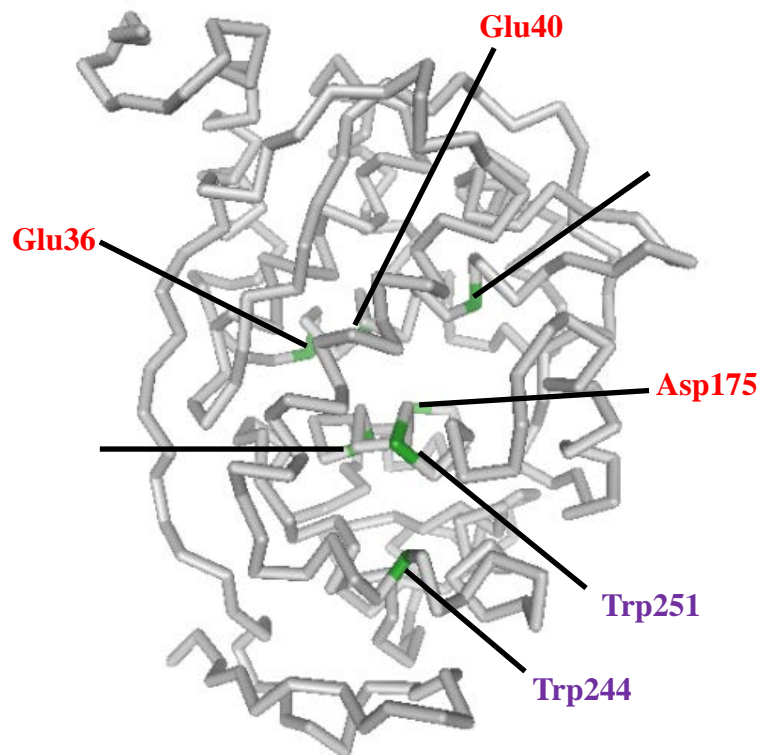
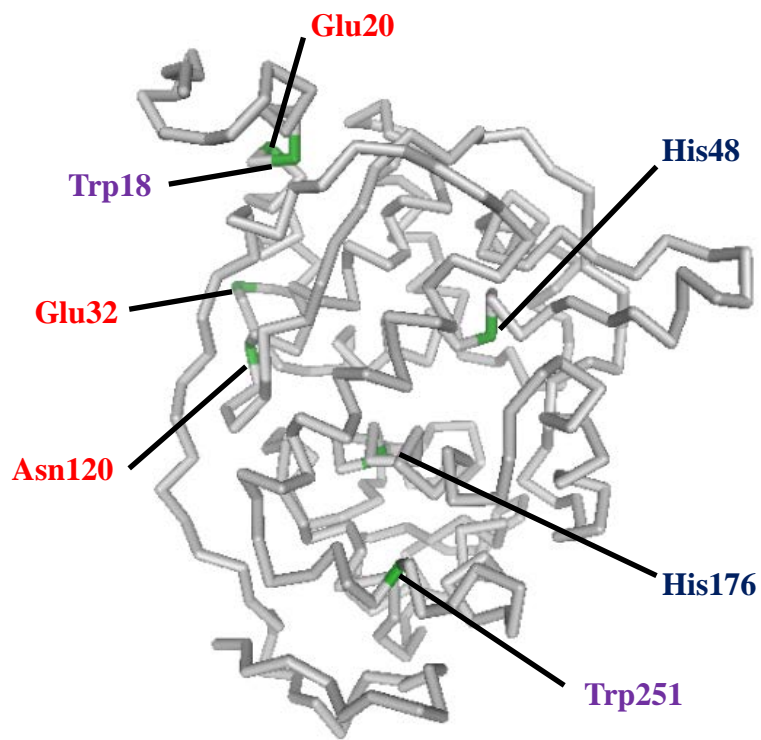
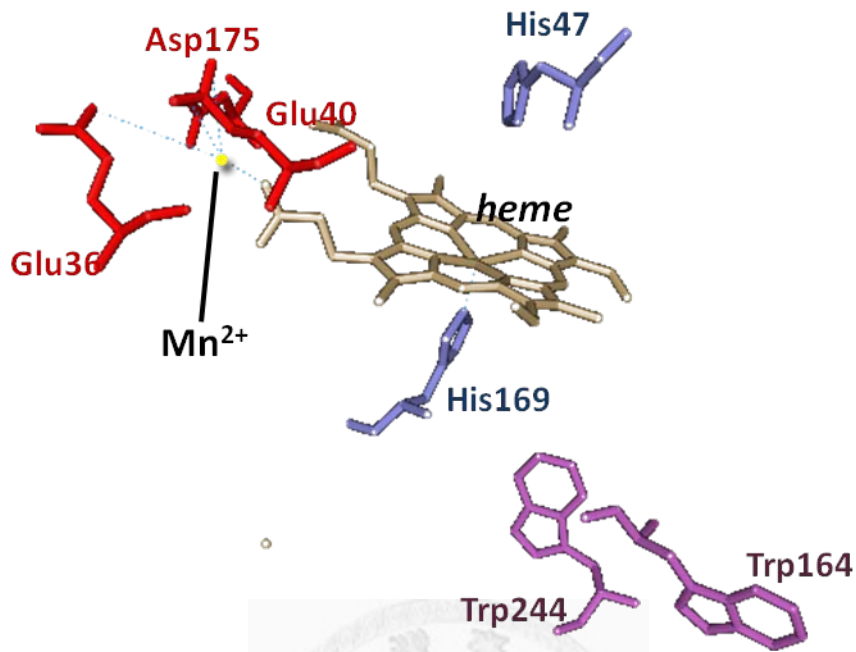


Fig. 9. The comparison of backbone structure between putative of LsBaP (up) and versatile peroxidase of *P. eryngii* (down) .

The protein structure of *P. eryngii* was retrieved from Protein Database Bank (PDB). (PDB id: 3FM1). (A) The putative modeling structure of LsLnP. Unclassical manganese binding site composed of Glu20, Glu32 and Asn120 is marked in red. Distal histidine (His48), proximal histidine (His176) and inappropriate locations of two tryptophan residues (Trp18 and Trp251) are marked in blue and purple respectively. (B) The protein structure of *P. eryngii*. Classical manganese binding site composed of Glu36, Glu40 and Asp175 are marked in red. Distal and proximal histidine (His47 and His169) are marked in blue; tryptophan residues (Trp244 and Trp251) constituting VA binding site are marked in purple.



A



B

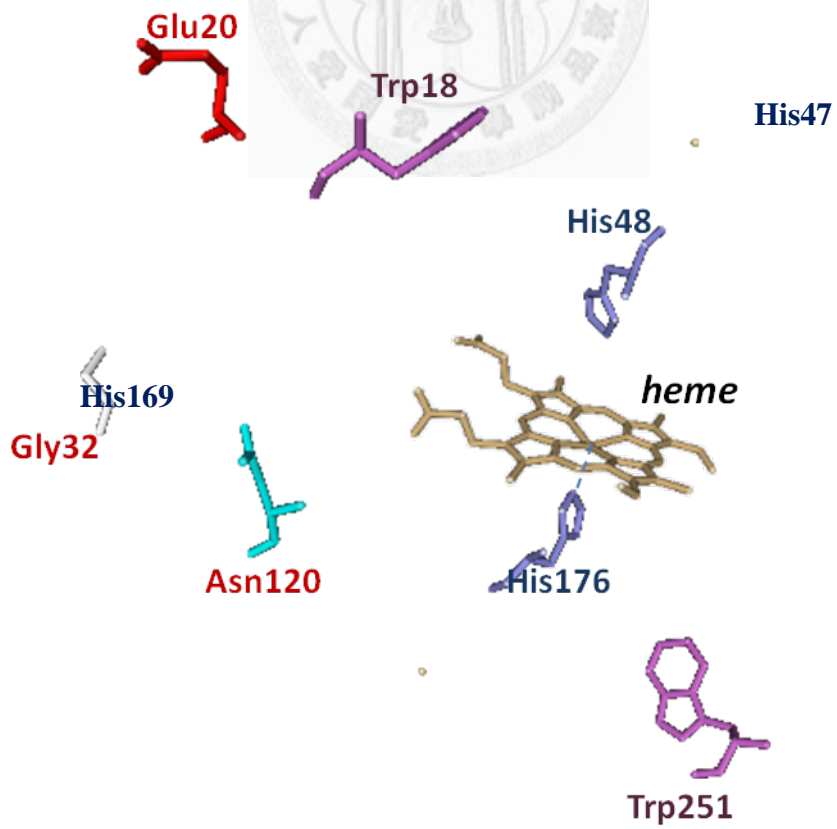


Fig. 10. The comparison of ligand binding site between *P. eryngii* versatile peroxidase and the *L. sulphureus* novel peroxidase.

(A) Versatile peroxidase of *P. eryngii*: Detail structure of heme pocket, a heme cofactor with distal histidine (His47, blue) and proximal histidine (His169, blue). Mn-oxidation site consist of Asp175, Glu36 and Glu40 (all in red) and Trp164 and Trp244 within VA binding site. (B) Detail structure of LsBaP. Heme pocket is composed of distal histidine (His48, blue) and proximal histidine (His176, blue). LsBaP lack of Mn binding site, two residues substituted by Asn120 (light blue) and Gly32 (gray). Trp18 and Trp251 (purple) are located on the sides of heme cofactor, lack VA binding site.



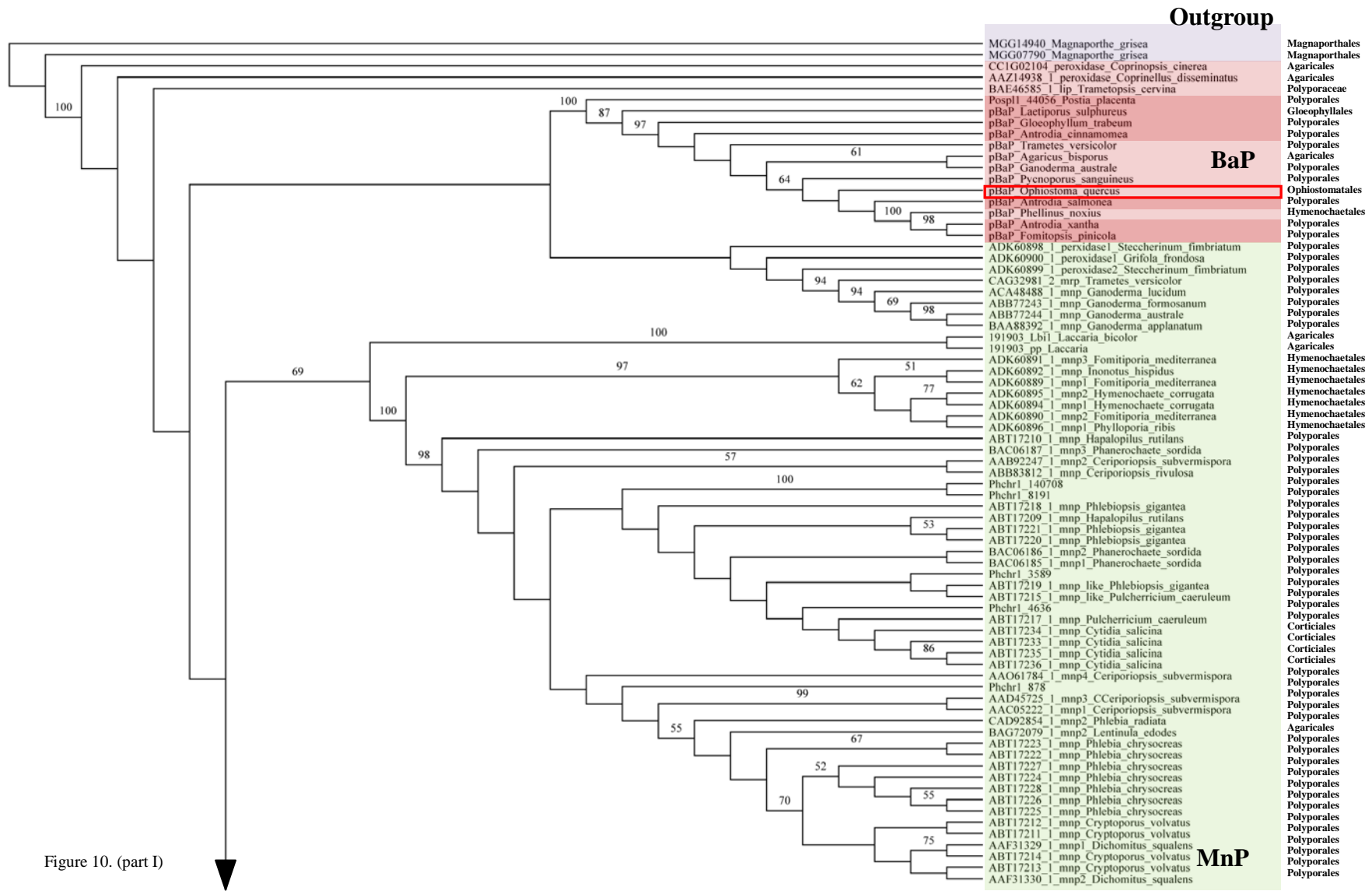


Figure 10. (part I)

Figure 10. (part II)

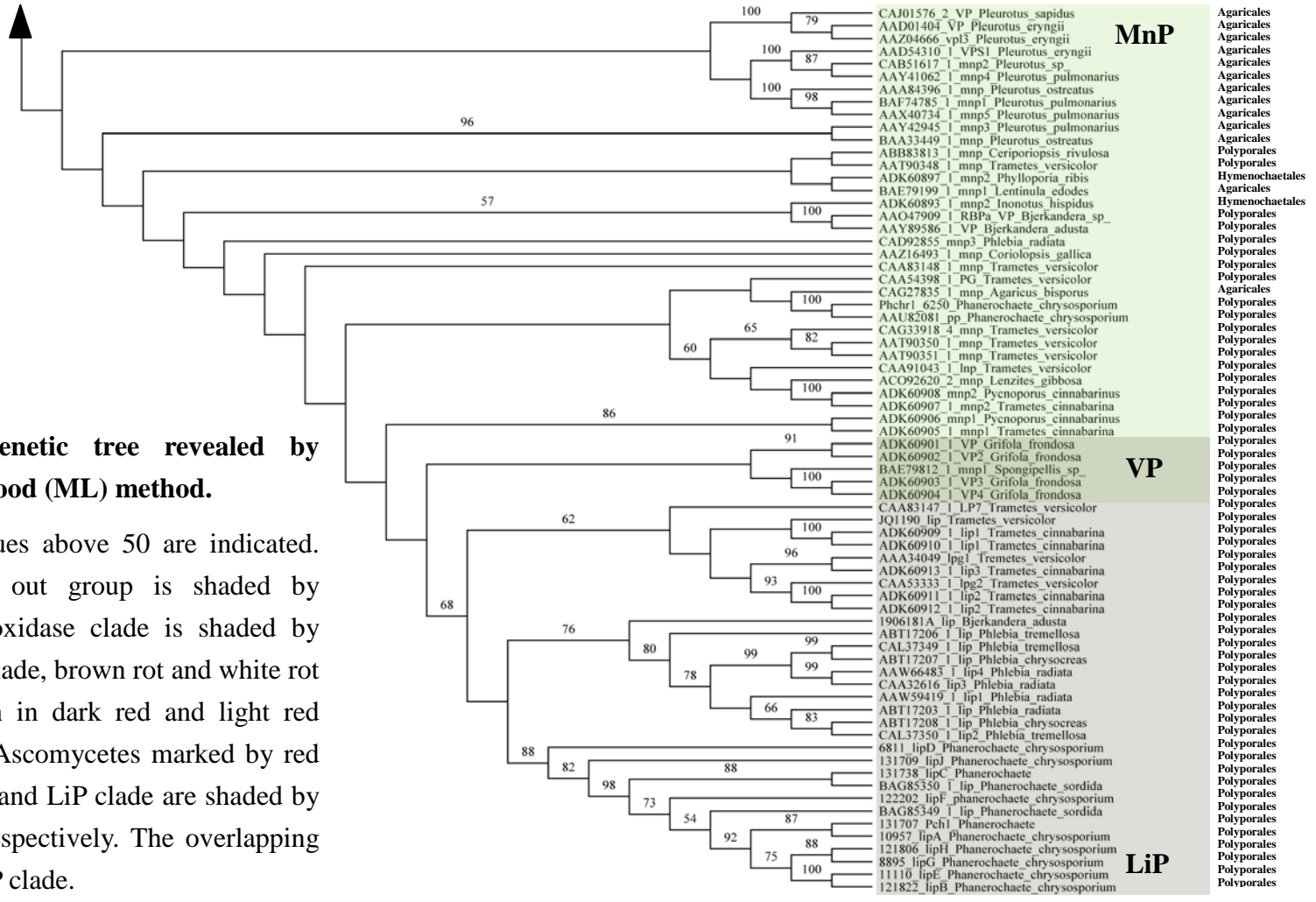


Fig. 11. Phylogenetic tree revealed by Maximum likelihood (ML) method.

ML bootstrap values above 50 are indicated. The Ascomycota out group is shaded by purple, basal peroxidase clade is shaded by red. Among BaP clade, brown rot and white rot species are shown in dark red and light red respectively; and Ascomycetes marked by red frame. MnP clade and LiP clade are shaded by green and blue, respectively. The overlapping zone represents VP clade.

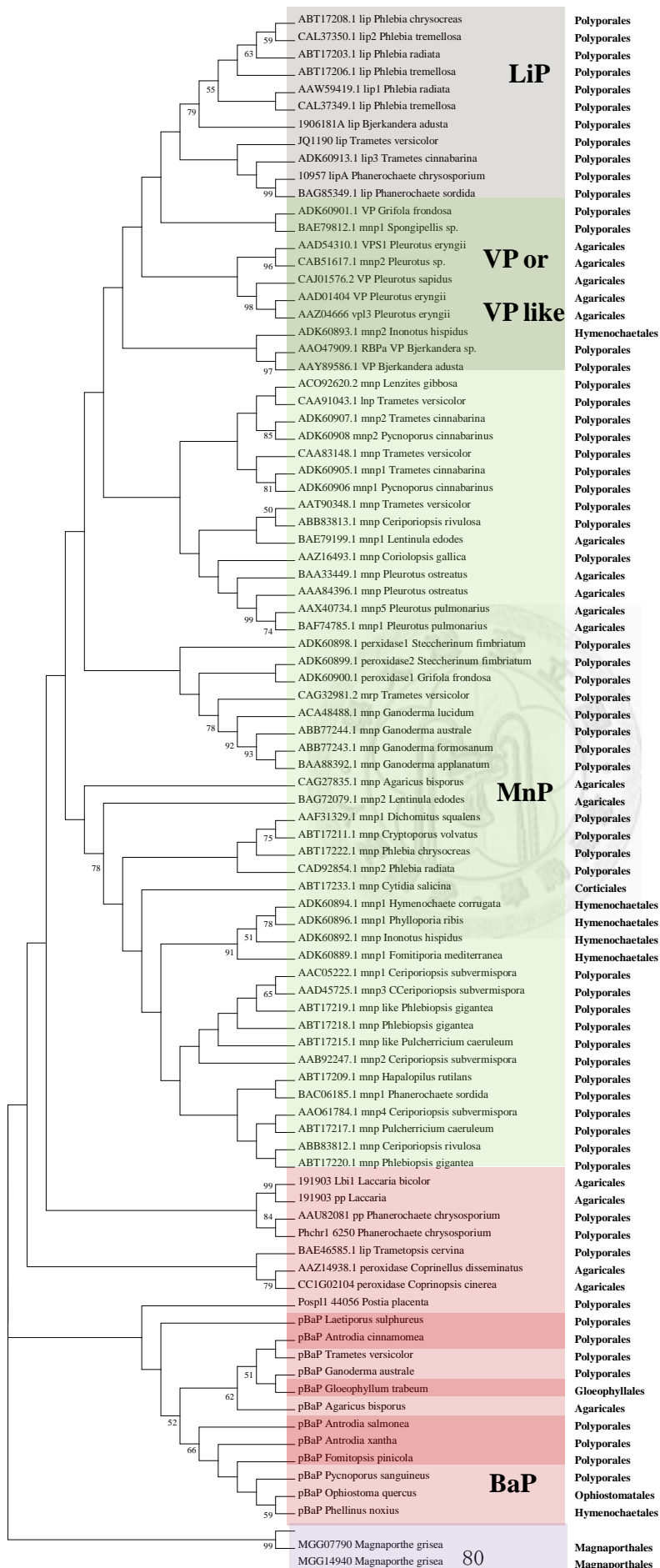


Figure 12. The Phylogenetic tree disclosed by Neighbor-joining (NJ) method.

NJ bootstrap values above 70 are indicated. Ascomycota out group is shaded by purple, basal peroxidase clade by red. Among BaP clades, brown rot and white rot species are shown in dark red and light red; MnP clade and LiP clade by green and blue, respectively. The overlapping zone represents VP clade.



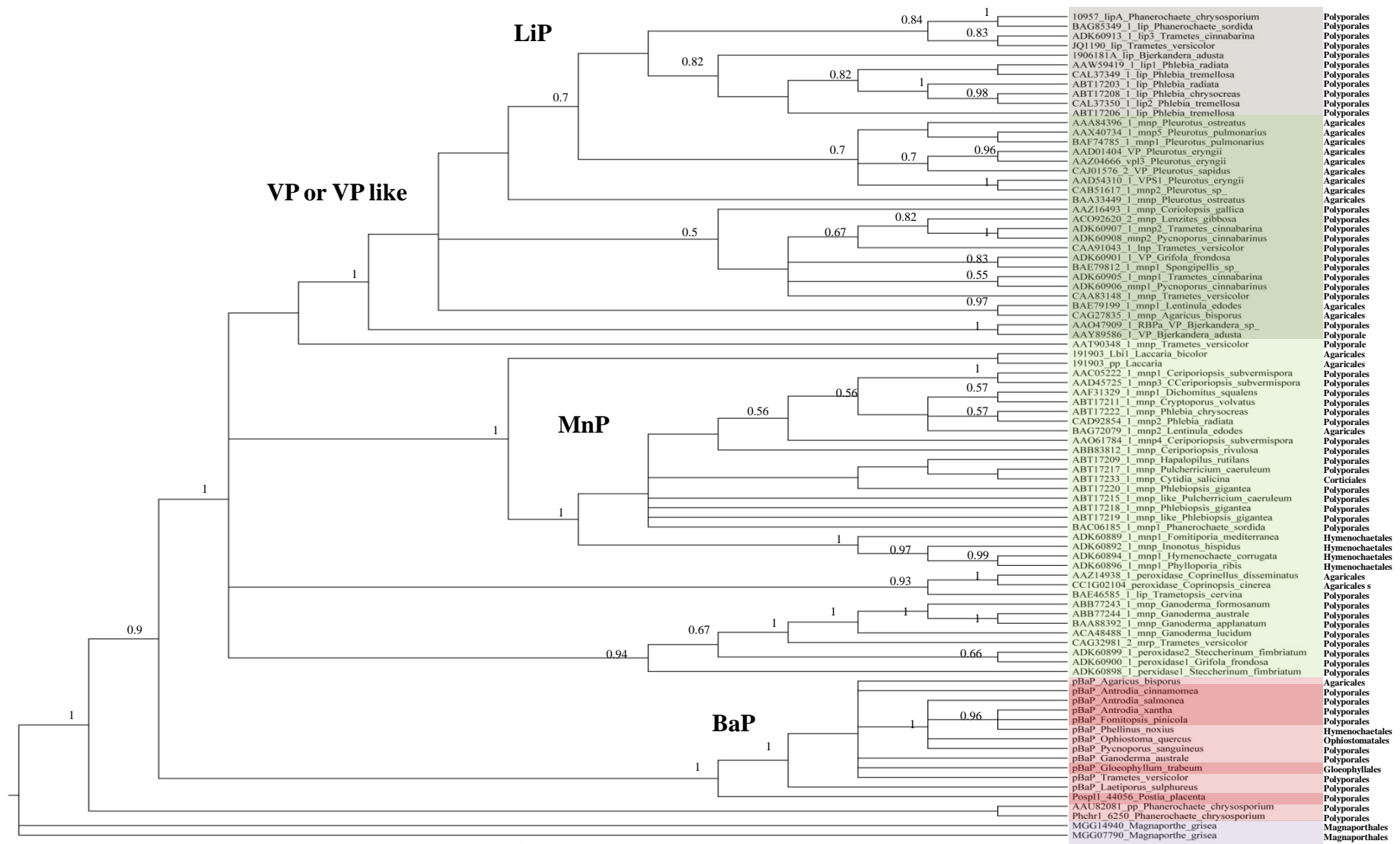


Figure 13. The phylogenetic tree showed by Bayesian inference (BI) method.

Bayesian posterior probability is indicated. Ascomycota out group is shaded by purple, Basal peroxidase clade by red. Among BaP clades, brown rot and white rot species are shown in dark red and light red, MnP clade and LiP clade by green and blue, respectively. The overlapping zone represents VP clade.



Appendix

Appx Table 1. Sequence used in the phylogenetic analysis

Accession no.	Species	Order	Group	Source
CAL37349	<i>Phlebia tremellosa</i>	Polyporales	LiP	GenBank
CAA32616	<i>Phlebia radiata</i>	Polyporales	LiP	(Saloheimo et al. 1989)
Pch1131738	<i>Phanerochaete chrysosporium</i>	Polyporales	LiP	(Martinez et al. 2004)
Pch1131709	<i>Phanerochaete chrysosporium</i>	Polyporales	LiP	(Martinez et al. 2004)
BAG85350	<i>Phanerochaete sordida</i>	Polyporales	LiP	(Sugiura et al. 2009)
Pch1122202	<i>Phanerochaete chrysosporium</i>	Polyporales	LiP	(Martinez et al. 2004)
CAL37350	<i>Phlebia tremellosa</i>	Polyporales	LiP	GenBank
AAW59419	<i>Phlebia radiata</i>	Polyporales	LiP	(Hilden et al. 2006)
Pch1121806	<i>Phanerochaete chrysosporium</i>	Polyporales	LiP	(Martinez et al. 2004)
Pch1 8895	<i>Phanerochaete chrysosporium</i>	Polyporales	LiP	(Martinez et al. 2004)
Pch111110	<i>Phanerochaete chrysosporium</i>	Polyporales	LiP	(Martinez et al. 2004)
Pch1 121822	<i>Phanerochaete chrysosporium</i>	Polyporales	LiP	(Martinez et al. 2004)
Pch1 6811	<i>Phanerochaete chrysosporium</i>	Polyporales	LiP	(Martinez et al. 2004)
BAG85349	<i>Phanerochaete sordida</i>	Polyporales	LiP	(Sugiura et al. 2009)
Pch1 10957	<i>Phanerochaete chrysosporium</i>	Polyporales	LiP	(Martinez et al. 2004)
ABT17225	<i>Phlebia chrysocreas</i>	Polyporales	MnP1	(Morgenstern et al. 2008)
AAF31330	<i>Dichomitus squalens</i>	Polyporales	MnP1	(Li et al. 1999)
AAO61784	<i>Ceriporiopsis subvermispota</i>	Polyporales	MnP1	(Sue Yaver et al. 2003)

ABB83812 Continued	<i>Ceriporiopsis rivulosa</i>	Polyporales	MnP1	(Hakala et al. 2006)
BAC06187	<i>Phanerochaete sordida</i>	Polyporales	MnP1	GenBank
ABT17210	<i>Hapalopilus rutilans</i>	Polyporales	MnP1	(Morgenstern et al. 2008)
Pch1 878	<i>Phanerochaete chryso sporium</i>	Polyporales	MnP1	(Martinez et al. 2004)
ABT17219	<i>Phlebiopsis gigantea</i>	Polyporales	MnP1	(Morgenstern et al. 2008)
ABT17215	<i>Pulcherricium caeruleum</i>	Polyporales	MnP1	(Morgenstern et al. 2008)
ABT17235	<i>Cytidia salicina</i>	Corticiales	MnP1	(Morgenstern et al. 2008)
ABT17233	<i>Cytidia salicina</i>	Corticiales	MnP1	(Morgenstern et al. 2008)
AAD45725	<i>Ceriporiopsis subvermispora</i>	Polyporale	MnP1	(Tello et al. 2000)
ABT17236	<i>Cytidia salicina</i>	Corticiales	MnP1	(Morgenstern et al. 2008)
ABT17228	<i>Phlebia chrysocreas</i>	Polyporale	MnP1	(Morgenstern et al. 2008)
AAC05222	<i>Ceriporiopsis subvermispora</i>	Polyporales	MnP1	(Lobos et al. 1998)
ABT17227	<i>Phlebia chrysocreas</i>	Polyporales	MnP1	(Morgenstern et al. 2008)
ABT17234	<i>Cytidia salicina</i>	Corticiales	MnP1	(Morgenstern et al. 2008)
AAB92247	<i>Ceriporiopsis subvermispora</i>	Polyporales	MnP1	GenBank
AAF31329	<i>Dichomitus squalens</i>	Polyporales	MnP1	(Li et al. 1999)
ABT17214	<i>Cryptoporus volvatus</i>	Polyporales	MnP1	(Morgenstern et al. 2008)
ABT17211	<i>Cryptoporus volvatus</i>	Polyporales	MnP1	(Morgenstern et al. 2008)
ABT17213	<i>Cryptoporus volvatus</i>	Polyporales	MnP1	(Morgenstern et al. 2008)
ABT17224	<i>Phlebia chrysocreas</i>	Polyporales	MnP1	(Morgenstern et al. 2008)
ABT17226	<i>Phlebia chrysocreas</i>	Polyporales	MnP1	(Morgenstern et al. 2008)

CAD92854 Continued	<i>Phlebia radiata</i>	Polyporales	MnP1	(Hildén et al. 2005)
BAG72079	<i>Lentinula edodes</i>	Agaricales	MnP1	(Sakamoto et al. 2009)
ABT17223	<i>Phlebia chrysocreas</i>	Polyporales	MnP1	(Morgenstern et al. 2008)
ABT17222	<i>Phlebia chrysocreas</i>	Polyporales	MnP1	(Morgenstern et al. 2008)
ABT17212	<i>Cryptoporus volvatus</i>	Polyporales	MnP1	(Morgenstern et al. 2008)
ADK60890	<i>Fomitiporia mediterranea</i>	Hymenochaetales	MnP1	(Morgenstern et al. 2010)
ADK60896	<i>Phylloporia ribis</i>	Hymenochaetales	MnP1	(Morgenstern et al. 2010)
ADK60894	<i>Hymenochaete corrugata</i>	Hymenochaetales	MnP1	(Morgenstern et al. 2010)
ADK60895	<i>Hymenochaete corrugata</i>	Hymenochaetales	MnP1	(Morgenstern et al. 2010)
ADK60892	<i>Inonotus hispidus</i>	Hymenochaetales	MnP1	(Morgenstern et al. 2010)
ADK60889	<i>Fomitiporia mediterranea</i>	Hymenochaetales	MnP1	(Morgenstern et al. 2010)
ADK60891	<i>Fomitiporia mediterranea</i>	Hymenochaetales	MnP1	(Morgenstern et al. 2010)
ADK60898	<i>Steccherinum fimbriatum</i>	Polyporales		(Morgenstern et al. 2010)
ADK60899	<i>Steccherinum fimbriatum</i>	Polyporales		(Morgenstern et al. 2010)
ADK60900	<i>Grifola frondosa</i>	Polyporales		(Morgenstern et al. 2010)
BAA88392	<i>Ganoderma applanatum</i>	Polyporales		GenBank
ABB77244	<i>Ganoderma australe</i>	Polyporales		GenBank
BAE46585	<i>Trametes cervina</i>	Polyporales		GenBank
ABB77243	<i>Ganoderma formosanum</i>	Polyporales		GenBank
ACA48488	<i>Ganoderma lucidum</i>	Polyporales		GenBank
AAU82081	<i>Phanerochaete chrysosporium</i>	Polyporales	NoP	(Martinez et al. 2004)
Pch1 6250	<i>Phanerochaete chrysosporium</i>	Polyporales	BaP	(Martinez et al. 2004)

AY243868 Continued	<i>Pycnoporus coccineus</i>	Polyporales	LiP	(Pointing et al. 2005)
CAG32981	<i>Trametes versicolor</i>	Polyporales		(Kim et al. 2005)
AAW66483	<i>Phlebia radiata</i>	Polyporales	LiP	(Hilden et al. 2006)
ABT17207	<i>Phlebia chrysocreas</i>	Polyporales	LiP	(Morgenstern et al. 2008)
ABT17206	<i>Phlebia tremellosa</i>	Polyporales	LiP	(Morgenstern et al. 2008)
ABT17208	<i>Phlebia chrysocreas</i>	Polyporales	LiP	(Morgenstern et al. 2008)
ADK60913	<i>Trametes cinnabarina</i>	Polyporales	LiP	(Morgenstern et al. 2010)
ABT17203	<i>Phlebia radiata</i>	Polyporales	LiP	(Morgenstern et al. 2008)
1906181A	<i>Bjerkandera adusta</i>	Polyporales	LiP	(Kimura et al. 1991)
ADK60911	<i>Trametes cinnabarina</i>	Polyporales	LiP	(Morgenstern et al. 2010)
ADK60912	<i>Trametes cinnabarina</i>	Polyporales	LiP	(Morgenstern et al. 2010)
AAA34049	<i>Trametes versicolor</i>	Polyporales	LiP	(Jonsson et al. 1992)
CAA53333	<i>Trametes versicolor</i>	Polyporales	LiP	(Jönsson et al. 1994)
ADK60909	<i>Trametes cinnabarina</i>	Polyporales	LiP	(Morgenstern et al. 2010)
ADK60910	<i>Trametes cinnabarina</i>	Polyporales	LiP	(Morgenstern et al. 2010)
JQ1190	<i>Trametes versicolor</i>	Polyporales	LiP	(Black et al. 1991)
CAA83147	<i>Trametes versicolor</i>	Polyporales	LiP	(Johansson et al. 1995)
Lb1191903	<i>Laccaria bicolor</i>	Agaricales	PP?	(Martin et al. 2008)
Pch1140708	<i>Phanerochaete chrysosporium</i>	Polyporales	MnP1	(Martinez et al. 2004)
Pch1 8191	<i>Phanerochaete chrysosporium</i>	Polyporales	MnP1	(Martinez et al. 2004)
ABT17217	<i>Pulcherricium</i>	Polyporales	MnP1	(Morgenstern

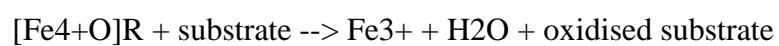
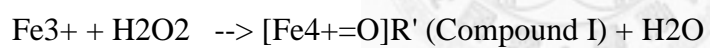
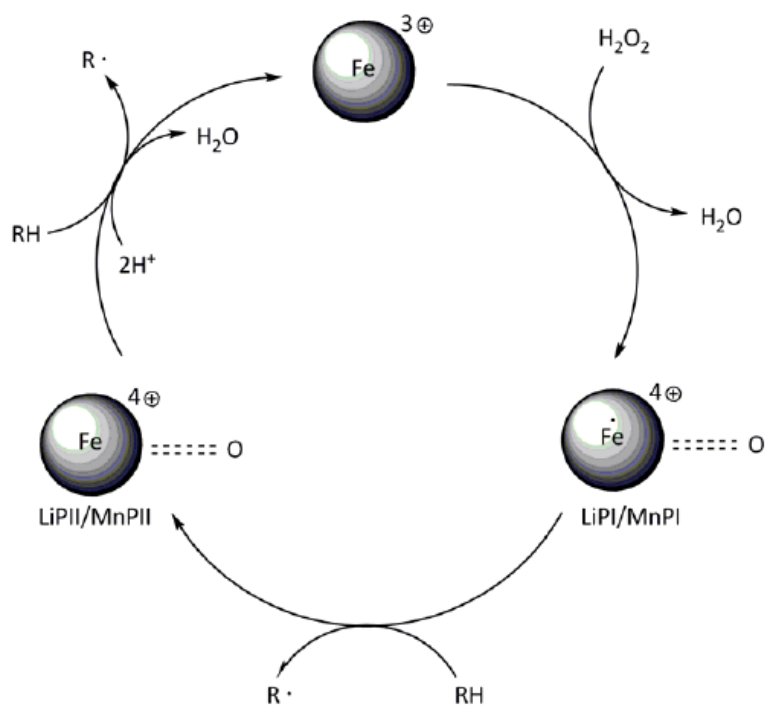
	<i>caeruleum</i>			et al. 2008)
ABT17209 Continued	<i>Hapalopilus rutilans</i>	Polyporales	MnP1	(Morgenstern et al. 2008)
ABT17220	<i>Phlebiopsis gigantea</i>	Polyporales	MnP1	(Morgenstern et al. 2008)
ABT17221	<i>Phlebiopsis gigantea</i>	Polyporales	MnP1	(Morgenstern et al. 2008)
ABT17218	<i>Phlebiopsis gigantea</i>	Polyporales	MnP1	(Morgenstern et al. 2008)
BAC06185	<i>Phanerochaete sordida</i>	Polyporales	MnP1	GenBank
Pch13589	<i>Phanerochaete chrysosporium</i>	Polyporales	MnP1	(Martinez et al. 2004)
BAC06186	<i>Phanerochaete sordida</i>	Polyporales	MnP1	GenBank
BAF74785	<i>Pleurotus pulmonarius</i>	Agaricales	VP1	GenBank
AAT90348	<i>Trametes versicolor</i>	Polyporales	MnP3	GenBank
AAY41062	<i>Pleurotus pulmonarius</i>	Agaricales	VP1	GenBank
CAB51617	<i>Pleurotus ostreatus</i>	Agaricales	VP1	(Giardina et al. 2000)
AAX40734	<i>Pleurotus pulmonarius</i>	Agaricales	VP1	GenBank
AAD54310	<i>Pleurotus eryngii</i>	Agaricales	VP1	(Camarero et al. 1999)
	<i>Gloeophyllum trabeum</i> ^a	Gloeophyllales	pBaP	This study
	<i>Agaricus bisporus</i>	Agaricales	pBaP	This study
	<i>Fomitopsis pinicola</i> ^a	Polyporales	pBaP	This study
	<i>Phellinus noxius</i>	Hymenochaetales	pBaP	This study
CC1G02104	<i>Coprinopsis cinerea</i>	Agaricales	BaP	genome site
AAZ14938	<i>Coprinellus disseminatus</i>	Agaricales	BaP	(James et al. 2006)
AAY89586	<i>Bjerkandera adusta</i>	Polyporales	VP3	GenBank
	<i>Antrodia xantha</i> ^a	Polyporales	pBaP	This study
	<i>Laetiporus sulphureus</i> ^a	Polyporales	pBaP	This study
	<i>Ophiostoma quercus</i> ^b	Ophiostomatales	pBaP	This study
Ppl144056	<i>Postia placenta</i> ^a	Polyporales	BaP	(Martinez et al.

				2009)
ABB83813 Continued	<i>Ceriporiopsis rivulosa</i>	Polyporales	MnP3	(Hakala et al. 2006)
CAA91043	<i>Trametes versicolor</i>	Polyporales	MnP4	GenBank
AAT90350	<i>Trametes versicolor</i>	Polyporales	MnP4	GenBank
	<i>Trametes versicolor</i>	Polyporales	pBaP	This study
AAO47909	<i>Bjerkandera sp.</i>	Polyporales	VP3	(Moreira et al. 2005)
	<i>Pycnoporus sanguineus</i>	Polyporales	BaP	This study
	<i>Antrodia salmonea</i> ^a	Polyporales	BaP	This study
	<i>Antrodia cinnamomea</i> ^a	Polyporales	BaP	This study
ADK60904	<i>Grifola frondosa</i>	Polyporales	VP2	(Morgenstern et al. 2010)
CAA54398	<i>Trametes versicolor</i>	Polyporales	MnP3	(Jönsson et al. 1994)
AAT90351	<i>Trametes versicolor</i>	Polyporales	MnP4	GenBank
CAG33918	<i>Trametes versicolor</i>	Polyporales	MnP4	GenBank
ACO92620	<i>Pseudotrametes gibbosa</i>	Polyporales	MnP4	GenBank
ADK60905	<i>Trametes cinnabarina</i>	Polyporales	MnP4	(Morgenstern et al. 2010)
ADK60907	<i>Trametes cinnabarina</i>	Polyporales	MnP4	(Morgenstern et al. 2010)
ADK60906	<i>Pycnoporus cinnabarinus</i>	Polyporales	MnP4	(Morgenstern et al. 2010)
AAZ16493	<i>Coriolopsis gallica</i>	Polyporales	MnP4	GenBank
CAD92855	<i>Phlebia radiata</i>	Polyporales	MnP4	(Hildén et al. 2005)
CAA83148	<i>Trametes versicolor</i>	Polyporales	MnP4	(Johansson et al. 2002)
ADK60908	<i>Pycnoporus cinnabarinus</i>	Polyporales	MnP4	(Morgenstern et al. 2010)
BAE79812	<i>Spongipellis.</i>	Polyporales	VP2	GenBank
ADK60902	<i>Grifola frondosa</i>	Polyporales	VP2	(Morgenstern et al. 2010)
ADK60901	<i>Grifola frondosa</i>	Polyporales	VP2	(Morgenstern et al. 2010)

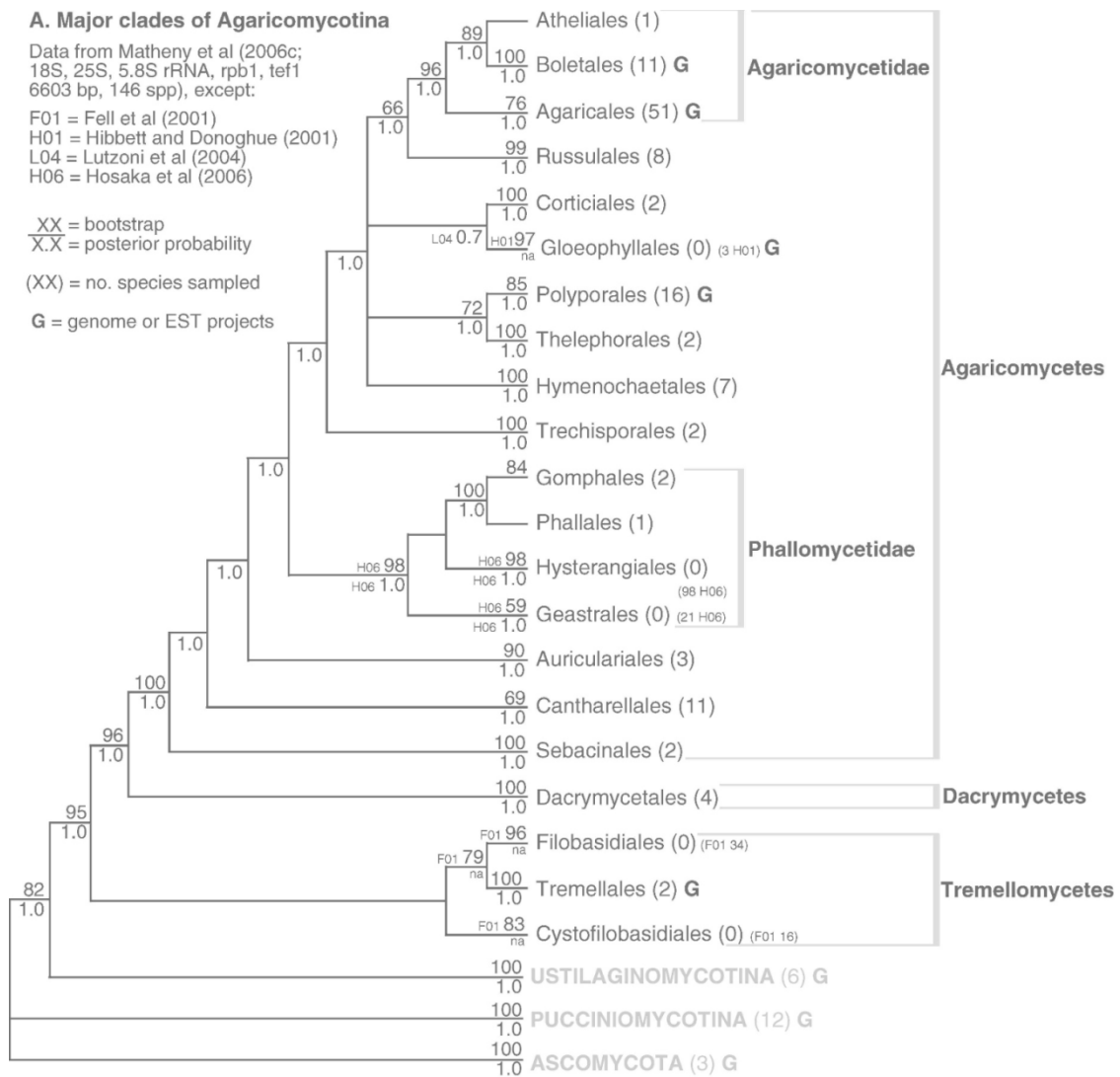
ADK60903	<i>Grifola frondosa</i>	Polyporales	VP2	(Morgenstern et al. 2010)
BAE79199 Continued	<i>Lentinula edodes</i>	Agaricales	MnP3	(Nagai et al. 2007)
AAA84396	<i>Pleurotus ostreatus</i>	Agaricales	VP1	(Asada et al. 1995)
AAZ04666	<i>Pleurotus eryngii</i>	Agaricales	VP1	GenBank
AAD01404	<i>Pleurotus eryngii</i>	Agaricales	VP1	(Ruiz-Dueñas et al. 1999)
CAJ01576	<i>Pleurotus sapidus</i>	Agaricales	VP1	GenBank
AAY42945	<i>Pleurotus pulmonarius</i>	Agaricales	MnP2	GenBank
BAA33449	<i>Pleurotus ostreatus</i>	Agaricales	MnP2	(Irie et al. 2000)
ADK60893	<i>Inonotus hispidus</i>	Hymenochaetales	MnP3	(Morgenstern et al. 2010)
CAG27835	<i>Agaricus bisporus</i>	Agaricales	MnP2	(Lankinen et al. 2005)
Pch1131707	<i>Phanerochaete chrysosporium</i>	Polyporales	LiP	(Martinez et al. 2004)
	<i>Ganoderma australe</i>	Polyporales	pBaP	This study
Pch14636	<i>Phanerochaete chrysosporium</i>	Polyporales	MnP1	(Martinez et al. 2004)
MGG07790	<i>Magnaporthe grisea</i> ^b	Magnaporthales	PP	(Dean et al. 2005)
MGG14940	<i>Magnaporthe grisea</i> ^b	Magnaporthales	PP	(Dean et al. 2005)

a. Brown rot fungi

b. Ascomycetes



Appx Fig. 1. The oxidation mechanism of LiP and MnP



Appx Fig. 2. Higher-level phylogenetic relationships of Agaricomycotina

Reference: Hibbett, D. S. (2006). A phylogenetic overview of the Agaricomycotina. *Mycologia*. 98(6): 917-925.